NACA

RESEARCH MEMORANDUM

A HORIZONTAL-TAIL ARRANGEMENT FOR COUNTERACTING STATIC LONGITUDINAL INSTABILITY OF SWEPTBACK WINGS

By George G. Edwards and Howard F. Savage

Ames Aeronautical Laboratory
Moffett Field, Calif.

CLASSIFIED DOCUMENT

NATIONAL ADVISORY COMMITTEE
FOR AERONAUTICS

WASHINGTON

May 25, 1956

NACA RM A56D06

NATIONAL ADVISORY COMMITTEE FOR AERONAUTICS

RESEARCH MEMORANDUM

A HORIZONTAL-TAIL ARRANGEMENT FOR COUNTERACTING STATIC LONGITUDINAL INSTABILITY OF SWEPTBACK WINGS

By George G. Edwards and Howard F. Savage

SUMMARY

An exploratory investigation has been made of the effectiveness of outboard horizontal tails in reducing the static longitudinal stability changes with lift coefficient associated with many sweptback wings. The horizontal-tail surfaces were mounted on booms extending rearward from approximately the mid-semispan of the wing. The objective was to place the horizontal tail in a region where favorable downwash changes occur concomitant with the adverse lift changes on the sweptback wing which cause losses in static longitudinal stability.

Tests were conducted on a semispan model wing and fuselage which, in a previous investigation, had been tested in combination with a conventional sweptback horizontal tail. In the present tests, outboard horizontal tails of several sizes were supported on booms from the wing in several longitudinal, vertical, and lateral positions. The wing had 45° sweepback and an aspect ratio of 6. Lift, drag, and pitching-moment data were measured through a Mach number range from 0.25 to 0.92 at a Reynolds number of 2,000,000 and at a Mach number of 0.25 at a Reynolds number of 8,000,000.

The results of the investigation indicate that outboard horizontal tails, properly positioned, can be a very effective means of counteracting the trend toward longitudinal instability which is characteristic of many sweptback wings at moderate to high lift coefficients. For one configuration tested, undesirable variations in longitudinal stability with lift coefficient were essentially eliminated. The results show that the effectiveness of this tail arrangement is, as expected, due to large and favorable downwash changes which increase the tail contribution to static longitudinal stability at the higher lift coefficients.

The test results indicate that properly positioned wing fences can be used to broaden the range of tail positions which produce acceptable

static longitudinal stability characteristics. The outboard tails were effective in reducing adverse changes in longitudinal stability of the configuration with an extended split flap.

INTRODUCTION

The achievement of satisfactory static longitudinal stability characteristics continues to be a major problem in the design of airplanes with sweptback wings, particularly when the wing has a moderate to high aspect ratio and sweepback of 45° or higher. Many of these wings develop static longitudinal instability at lift coefficients less than the maximum even with fixes such as fences, vortex generators, or leading-edge discontinuities (see, e.g., refs. 1 and 2). For these cases, good static longitudinal stability characteristics with tail on require a compensating increase in the stability contribution of the horizontal tail to offset the loss of longitudinal stability of the wing with increasing lift coefficient. The conventional fuselage-mounted tail is in a poor position to accomplish this since the required downwash changes do not occur behind the root sections of the sweptback wing (these sections are the last to suffer a reduction in lift-curve slope because of effective boundary-layer control resulting from spanwise drainage of boundary-layer air). On the other hand, favorable downwash changes may be expected behind the outer sections of the sweptback wing as a result of the decreases in lift-curve slope of these sections, which are, in fact, the usual cause of the deteriorating longitudinal stability of the wing (e.g., see ref. 3). A horizontal tail located well outboard of the fuselage should function to offset decreasing longitudinal stability of the wing through a decrease in the rate of change of downwash with angle of attack.

The airplane configuration resulting from the above considerations has the horizontal-tail surfaces mounted on booms extending rearward from approximately the mid-semispan of the wing. To the designer, this arrangement poses rigorous structural problems and perhaps a penalty in wing weight to insure adequate rigidity. However, the outboard tail arrangement offers a number of interesting design possibilities which seemed to make it worthy of consideration. For example, if vertical- as well as horizontal-tail surfaces were mounted on tail booms, the requirements for fuselage length and usage would be liberalized. This might also improve the directional characteristics at high angles of attack in cases where the effectiveness of the fuselage-mounted vertical surface is adversely affected by shed vorticity from the fuselage. The tail booms could provide valuable storage volume, at least in the forward portion, for such items as landing gear, fuel, or armament, and the accompanying increase in moment of inertia about the longitudinal axis would in some cases help to alleviate the critical yaw-roll coupling that might be encountered at high rates of roll due to low moments of inertia about the longitudinal axis. For some applications the booms might be arranged to improve the

longitudinal distribution of cross-sectional area and the moment of area for decreased drag at sonic and supersonic speeds. Consideration might also be given to the possibility of differentially controlling the horizontal-tail surfaces to provide lateral control even when the outer wing sections are stalled (ailevators). For some applications, the horizontal-tail surfaces may be needed only for improving longitudinal stability during take-off and landing; perhaps they could be rotated into the vertical plane to improve directional stability at high speeds. These examples illustrate that moving the tail surfaces from the fuselage to an outboard position extends the range of design possibilities.

An exploratory investigation has been conducted in the Ames 12-foot pressure wind tunnel to study some of the aerodynamic possibilities of outboard horizontal-tail surfaces, particularly in regard to their effectiveness in preventing static longitudinal instability of a sweptback wing-fuselage-tail configuration. Existing model parts, including a semispan model wing having 45° sweepback and an aspect ratio of 6, were utilized to form an airplane-like configuration. The wing had been tested previously with a fuselage and a conventional sweptback horizontal tail in the investigation of reference 1. The test conditions duplicated those of the reference to permit direct comparisons of data, covering a Mach number range up to 0.92 at a Reynolds number of 2,000,000 and including tests at a Reynolds number of 8,000,000 at a Mach number of 0.25. The horizontal-tail surfaces were supported on booms extending rearward from the wing, providing for variation of tail height, distance behind the wing, spanwise position, and tail incidence. Tail surfaces of three different sizes were tested. The tests also included a limited investigation of the effects of wing fences and of an extended split flap deflected 30.7°.

NOTATION

A	aspect ratio, $\frac{b^2}{2S}$
a	mean-line designation, fraction of chord over which design load is uniform
a_t	lift-curve slope of the isolated horizontal tail, per deg
a_{w+f+t}	lift-curve slope of the wing-fuselage-tail combination, per deg
$\frac{b}{2}$	wing semispan perpendicular to the plane of symmetry
C_D	drag coefficient, $\frac{\text{drag}}{qS}$
C_L	lift coefficient, $\frac{\text{lift}}{qS}$

[redacted]

C_m pitching-moment coefficient about the quarter point of the wing mean aerodynamic chord, $\frac{\text{pitching moment}}{qS\bar{c}}$

C_{m_α} rate of change of pitching-moment coefficient with angle of attack

c local wing chord parallel to the plane of symmetry

c' local wing chord perpendicular to the wing sweep axis

$\bar{c}$ mean aerodynamic chord, $\frac{\int_0^{b/2} c^2 dy}{\int_0^{b/2} c\, dy}$

c_{l_i} section design lift coefficient

i_t incidence of the horizontal tail with respect to the root chord of the wing

l_t tail length, longitudinal distance between the quarter points of the mean aerodynamic chords of the wing and the horizontal tail

M free-stream Mach number

q free-stream dynamic pressure

R Reynolds number based on the mean aerodynamic chord of the wing

S area of semispan wing

S_t area of semispan horizontal tail

t maximum thickness of section

$\bar{V}_t$ horizontal-tail volume coefficient, $\frac{S_t l_t}{S_w \bar{c}_w}$

y lateral distance from the plane of symmetry

z perpendicular distance from the plane of the wing-root chord and leading edge to the horizontal-tail hinge axis

α angle of attack of the wing-root chord

ϵ effective average downwash angle

φ angle of local wing chord relative to the wing-root chord, positive for washin, measured in planes parallel to the plane of symmetry

$\frac{\eta_t q_t}{q}$ tail efficiency factor (ratio of the lift-curve slope of the horizontal tail when mounted on the fuselage in the flow field of the wing to the lift-curve slope of the isolated horizontal tail)

Subscripts

f fuselage

t horizontal tail

w wing

MODEL

The model tested was constructed largely from existing parts and in no way represents an attempt to simulate an optimum design. The semispan wing and fuselage were those used in the investigation of reference 1 in which a conventional sweptback horizontal tail was mounted on the fuselage.

Details of the geometry of the model are given in figure 1 and in table I. Photographs of the model mounted in the wind tunnel are shown in figure 2. The wing had 45° of sweepback, an aspect ratio of 6, a taper ratio of 0.40, and NACA four-digit sections with camber and twist. The boundary-layer fences used with some of the outboard tail configurations extended from the trailing edge over the upper surface and around the leading edge of the wing to 0.10 chord on the lower surface (see fig. 1(b)). However, where data from reference 1 are used herein for comparative purposes, it should be noted that the fences lacked the section of fence extending around the leading edge from 0.10 chord on the upper surface to 0.10 chord on the lower surface, as indicated in figure 1(b).

The booms for mounting the horizontal tail were constructed of solid steel and had an elliptical cross section with a major axis of 4 inches and a minor axis of 1 inch. The booms were attached to the upper surface of the wing at either 0.4 b/2 or 0.5 b/2. Fairings were used at the juncture of the boom and wing surface (see figs. 1(b) and 2). Three booms were used to provide variations in tail length, tail height, and spanwise location (see fig. 1).

Horizontal-tail surfaces of three sizes were used. They are referred to throughout the report as "large," "medium," or "small," since the principal difference between them was size. The geometric properties of the three horizontal tails are given in table I and figure 1. The area of the large outboard tail was 83 percent of the conventional sweptback tail used in the investigation of reference 1.

The extended split flaps consisted of 1/8-inch-thick aluminum plates attached to the trailing edge of the wing. The flaps were supported by fixed brackets from the lower surface of the wing, had a chord equal to 20 percent of the wing chord measured parallel to the plane of symmetry, and were deflected 30.7° measured relative to the local chord in planes parallel to the plane of symmetry. The flaps extended spanwise from the fuselage to either 0.50 b/2 or 0.75 b/2. The gaps between the flap and the wing trailing edge and the fuselage were sealed.

CORRECTIONS TO DATA

The data have been corrected for constriction effects due to the presence of the tunnel walls (ref. 4), for tunnel-wall interference originating from lift on the model, and for drag tares caused by aerodynamic forces on the exposed portion of the turntable upon which the model was mounted.

Corrections for effects of tunnel-wall interference originating from the lift on the model were calculated by the method of reference 5. The corrections to the angle of attack and to the drag coefficient showed insignificant variation with Mach number. The corrections added to the data were as follows:

$$\Delta\alpha = 0.435\ C_L$$

$$\Delta C_D = 0.0068\ C_L^2$$

The corrections to the pitching-moment coefficient had significant variations with Mach number. The following corrections were added to the pitching-moment coefficients:

$$\Delta C_{m_{\text{tail off}}} = K_1 C_{L_{\text{tail off}}}$$

$$\Delta C_{m_{\text{tail on}}} = K_1 C_{L_{\text{tail off}}} - (K_2 C_{L_{\text{tail off}}} - \Delta\alpha)\frac{\partial C_m}{\partial i_t}$$

The values of K_1 and K_2 for each Mach number were calculated by the method of reference 5 and are given in the following table:

M	K_1	K_2
0.25	0.0024	0.64
.60	.0029	.67
.80	.0043	.71
.86	.0048	.73
.90	.0052	.76
.92	.0055	.77

Since the turntable upon which the model was mounted was directly connected to the balance system, a tare correction to the drag was necessary. This correction was determined by measuring the drag force on the turntable with the model removed from the wind tunnel.

TESTS

Test conditions were chosen to match those of previous tests of this model with a conventional sweptback tail (see ref. 1). Lift, drag, and pitching moment were measured for a large range of angles of attack at Mach numbers up to 0.92 at a Reynolds number of 2,000,000 and at a Mach number of 0.25 at a Reynolds number of 8,000,000. The first part of the investigation was conducted with the large outboard tail mounted in various longitudinal, lateral, and vertical positions. Tests were then conducted with the most satisfactory configurations to establish the effects of wing fences. The angle of incidence of the large horizontal tail was varied from -4° to -10° for one of the best configurations to provide the data required for computation of average downwash. To establish the effects of tail size on the pitching-moment characteristics, the model was also tested with horizontal tails having approximately three-fourths and one-half the area of the large tail.

The effects of extended split flaps on the longitudinal characteristics of various wing-fuselage-tail combinations were investigated at a Mach number of 0.25 and a Reynolds number of 8,000,000. The configurations tested included variations in flap span and in tail size, position, and incidence.

RESULTS AND DISCUSSION

Since the objective of the present investigation was to demonstrate certain principles and characteristics of outboard horizontal tails, it was not considered necessary to cover the entire range of possible tail positions nor to attain an optimum configuration. In fact, as has already

been pointed out, the model in no way represents an attempt to simulate an optimum design. In the presentation of the results, principal attention has been focused on the pitching-moment characteristics, since the lift characteristics are little affected by tail position and the drag of the outboard tail configuration must necessarily be evaluated in relation to the useful volume of both fuselage and tail booms.

Effects of Changes in Horizontal-Tail Position

The pitching-moment characteristics of the model with the large outboard tail in the low position behind the mid-semispan of the wing are presented in figure 3 for a range of Mach numbers. For comparison, similar data obtained in the investigation of reference 1 are presented for the model with a conventional fuselage-mounted tail, without wing fences and with the best four-fence configuration. These data indicate that the outboard tail is effective in preventing or delaying to higher lift coefficients the unstable trend of pitching-moment coefficients. In the following tabulation based on the data of figure 3, the approximate lift coefficient at which the unstable trend of pitching-moment coefficient with lift coefficient occurred is tabulated for each of the three configurations shown.

M	R	Conventional tail no wing fences	Conventional tail four wing fences	Outboard tail no wing fences
0.25	8,000,000	0.80	1.16	1.14
.80	2,000,000	.50	.84	1.00
.90	2,000,000	.40	.70	at least 0.93

As will be pointed out later, the decrease of longitudinal stability occuring for the outboard tail configuration at the lift coefficients listed above was probably caused by incipient stalling of the tail rather than by adverse downwash effects at the tail. The change in longitudinal stability at extreme negative lift coefficients is believed to be the result of stalling of the wing tip rather than stalling of the tail.

The investigation included tests of the model with the large outboard tail mounted in several other positions, all without the use of wing fences. The pitching-moment results are presented in figure 4. The effects of changing the height of the outboard tail as indicated in figure 4(a) are small but perceptible, the principal effect being to alter dC_m/dC_L at approximately the lift coefficient for which the wing itself begins to lose longitudinal stability. In this respect the pitching-moment

characteristics of the model with the outboard tail in the low position ($2z/b = 0$) appear to be slightly superior to those with the tail in the high position ($2z/b = 0.15$).

A change in the longitudinal position of the outboard tail ($l_t/\bar{c}_w = 2.61$ to $l_t/\bar{c}_w = 2.02$) produced the expected changes in static margin and some change in trim as may be seen in figure 4(b). There is some indication that moving the tail closer to the wing caused a slight reduction in the effectiveness of the outboard tail in preventing the unstable trend of pitching-moment coefficients.

The effects of moving the outboard tail from lateral position 0.5 b/2 to 0.4 b/2 are adverse as may be seen in figure 4(c). This result is in agreement with expectations based on the known tendency of the outer portions of the wing to stall first. The trend toward instability of the configuration with the outboard tail at 0.4 b/2 extends only over a small range of lift coefficients for which the flow separation on the wing is apparently concentrated too far out on the wing to materially change the downwash at the tail.

Effects of Wing Fences

The wing fence has often been used on sweptback wings as a means of delaying the trend toward longitudinal instability with increasing lift coefficient. In the investigation of reference 1, the present wing was tested with four fences with results as shown in figure 5. Considerable improvement is evident in the pitching-moment characteristics of the wing-fuselage combination due to the addition of fences. The effectiveness of the tail boom as a fence is demonstrated in figure 5 where the pitching-moment characteristics of the wing without fences but with the tail boom mounted at lateral position 0.5 b/2 are shown. The figure indicates that the effectiveness of the tail boom in reducing the unstable trend of pitching-moment coefficients was about half that of four fences.

In reference to the data of figure 4, it has been noted that with the outboard horizontal tail in some positions, objectionable changes in dC_m/dC_L occurred over a small range of lift coefficients near that at which the wing itself began to lose static longitudinal stability. The outboard tail, in contrast to a conventional fuselage-mounted tail, is in a portion of the flow field which may be changed materially by the action of a wing fence or other device which changes the wing load distribution. Therefore, a brief investigation of the effects of fences on the pitching-moment characteristics of the model with outboard tail was made.

With the large outboard tail mounted in the most favorable position according to figure 4 (in the low, most rearward position at lateral position 0.5 b/2), runs were made with a fence located successively at 0.65,

0.75, and 0.85 b/2. The objective was to obtain some small improvements in longitudinal stability characteristics in the range of lift coefficients from about 0.60 to 0.70. The results shown in figure 6 indicate that of the three fence positions tried, the one at 0.75 b/2 is most favorable.

With the outboard tail in the high position ($2z/b = 0.15$), the undesirable variations in longitudinal stability with lift coefficient were more pronounced than with the outboard tail in the low position, as is evident from figure 4(a). Figure 7 shows that a single wing fence at 0.75 b/2 produced pitching-moment characteristics with the high outboard tail which were almost as good as those with the low outboard tail.

Wing fences also produced large improvements in the pitching-moment characteristics of the model with the outboard tail at the more inboard lateral position (0.4 b/2). This can be seen in figure 8 where the pitching-moment characteristics with the tail in this position and with either one or two wing fences are compared with those obtained with fences removed. Also shown are the results for the most favorable outboard tail position. With the outboard tail located at lateral position 0.40 b/2, a single fence located at 0.65 b/2 seems to be sufficient to eliminate the loss of static longitudinal stability which occurred at lift coefficients of the order of 0.6 without wing fences. It would appear that the action of the fence in this case is to delay the reduction of lift-curve slope on the sections near the wing tip to higher lift coefficients and thereby insure that when the wing sections do begin to lose lift-curve slope, sections sufficiently far inboard will be affected and cause favorable changes in downwash at the tail.

In summary, the results of the tests with outboard tails and wing fences indicate that minor variations in the rate of change of pitching-moment coefficient with lift coefficient, which occurred for some positions of the tail, could be eliminated by the addition of a single fence to the wing. The range of acceptable outboard tail positions can thus be increased by the judicious use of wing fences.

Average Downwash at the Tail

The concept of placing the tail outboard is based on the likelihood that large and favorable changes of downwash occur behind the outer sections of a sweptback wing concomitant with decreasing static longitudinal stability of the wing itself. A decrease in the rate of change of downwash with angle of attack, $d\epsilon/d\alpha$, would increase the tail contribution to static longitudinal stability, as may be observed in the following expression for the tail contribution to the rate of change of pitching-moment coefficient with lift coefficient:

[redacted]

$$\left[\left(\frac{dC_m}{dC_L}\right)_t\right]_{w+f+t} = -\bar{V}_t \frac{a_t}{a_{w+f+t}} \left[\eta_t \frac{q_t}{q}\left(1 - \frac{d\epsilon}{d\alpha}\right) + \alpha_t \frac{\partial\left(\eta_t \frac{q_t}{q}\right)}{\partial\alpha}\right] \quad (1)$$

In order to investigate the average downwash changes, the pitching-moment characteristics of the model for one outboard tail configuration were measured with the tail set at four angles of incidence and with the tail removed. These data are presented in figure 9 for several Mach numbers. The average downwash at the tail was calculated from these data using the expression

$$\epsilon = \alpha + i_t - \frac{\left(C_{m_{\text{tail on}}} - C_{m_{\text{tail off}}}\right)_{\alpha = \text{constant}}}{\partial C_m / \partial i_t} \quad (2)$$

The downwash parameter $(1 - d\epsilon/d\alpha)$ was then determined from plots of ϵ versus α.

The relation between the total pitching-moment coefficients, pitching-moment coefficients due to the tail, and the downwash parameter $(1 - d\epsilon/d\alpha)$ may be observed in figure 10 where these quantities are plotted versus angle of attack. Data for the model with outboard tail in the low position at spanwise station 0.5 b/2 and with one wing fence are compared with those for the model with the conventional sweptback tail configuration using four wing fences. The total pitching-moment coefficients for the tail-off condition are also presented as a guide to flow conditions on the wing. The low-speed data of figure 10(a) indicate only small variations in the rate of change of pitching-moment coefficient with angle of attack, C_{m_α}, for the tail-off condition and, as might therefore be expected, little change in the downwash parameter $(1 - d\epsilon/d\alpha)$. At the higher Mach numbers, however, large increases in C_{m_α} occurred at moderate to high angles of attack for the tail-off condition. It may be seen from figures 10(b), 10(c), and 10(d) that the longitudinal stability characteristics of the configuration with outboard tail did not deteriorate because of compensating increases in the tail contribution to longitudinal stability (see eq. (1)) originating from decreases in $d\epsilon/d\alpha$ as evidenced in the plot of $(1 - d\epsilon/d\alpha)$. In contrast, the conventional sweptback tail failed to compensate for the poor longitudinal stability characteristics of the wing-fuselage configuration because the required downwash changes did not occur.

Theoretical estimates of the downwash at the tail at high angles of attack are not likely to be reliable because of the existence of separated flow on the wing. Such calculations based on an adaptation of the method of reference 6 gave poor results when based on a theoretical span load

distribution and only somewhat better results based on estimated span load distributions allowing for the effects of flow separation on the wing. Since actual surface pressure data were not available for this wing, it is not possible to state whether satisfactory estimates of downwash could be made on the basis of such data.

Effects of Changing Tail Size

According to equation (1) the tail contribution to static longitudinal stability is proportional to both tail area and $(1 - d\epsilon/d\alpha)$, neglecting the changes in average downwash at the tail which must obviously result from changing the extent of the tail in a nonuniform downwash field. To investigate the effects of changing tail size, outboard horizontal tails having approximately the same plan form as the large outboard tail but with tail areas approximately three-fourths and one-half of the large tail were tested in the most favorable position established by the tests with the large tail. The pitching-moment data obtained at several Mach numbers are presented in figure 11 for the model with each of the three outboard tails and with no tail, together with similar data for the model with a conventional fuselage-mounted tail. It should be noted that the area of the large outboard tail was 83 percent of the area of the conventional fuselage-mounted tail. The data of figure 11 indicate that even with the smallest of the three outboard tails (tail area 39 percent of that of the conventional tail), the pitching-moment characteristics are as good as or better than those with the conventional fuselage-mounted tail. With the smallest outboard tail there was some trend toward longitudinal instability in the range of lift coefficients from 0.6 to 0.7 at Mach numbers of 0.86 and 0.90, which did not occur for the larger tails. Presumably this was due to the effective inboard displacement of the tail as the tail span was reduced and could be remedied by changing the position of the wing fence, by adding another fence, or by moving the tail farther outboard.

In figure 12 $\left(C_{m_{\text{tail on}}} - C_{m_{\text{tail off}}}\right)$, derived from the data of figure 11, is plotted as a function of tail-volume coefficient $\bar{V}_t$ for various constant angles of attack. The pitching-moment coefficient due to the tail is indicated to be very nearly a linear function of tail-volume coefficient which, for constant tail length, l_t, is directly proportional to tail area. This means also that the tail contribution to static longitudinal stability $\left[(dC_m/dC_L)_t\right]_{w+f+t}$ is nearly proportional to tail area.

Most of the pitching-moment data for the model with the large outboard tail have shown a rather large increase in longitudinal stability, beginning at about the lift coefficient at which the longitudinal stability

of the wing-fuselage combination begins to decrease. For a constant value of dC_m/dC_L throughout the lift range, then, it is apparent that the large outboard tail overcompensated for the reduction of longitudinal stability of the wing-fuselage combination. It may be seen in figure 11 that one of the important effects of reducing tail area was to decrease this difference between dC_m/dC_L at high lift coefficients and that at low lift coefficients. The effect is shown more clearly in figure 13 where pitching-moment data for the large outboard tail configuration are shown for the moment center at both $0.25\bar{c}$ and $0.40\bar{c}$ compared to similar data for the small tail configuration with moment center at $0.25\bar{c}$.

Summarizing the foregoing discussion, it is concluded that for a given position of the outboard horizontal tail, the degree of static longitudinal stability at lift coefficients above that for pitch instability of the wing was approximately a linear function of tail size. The degree of stability in this high-lift range relative to that in the low-lift range could be adjusted by changing the horizontal-tail size. To the extent that these results can be generalized, it may be concluded that for any particular variations of $(dC_m/dC_L)_{\text{tail off}}$ and of $(1 - d\epsilon/d\alpha)$ with angle of attack, there is a tail-volume coefficient that will produce minimum change of $(dC_m/dC_L)_{\text{tail on}}$ with angle of attack.

Lift, Drag, and Pitching-Moment Characteristics

The lift, drag, and pitching-moment data for one outboard tail configuration are presented in figure 14 for the complete range of Mach numbers and Reynolds numbers. The lift and drag data are presented as a matter of interest only and have little significance in the present exploratory investigation. Within the range of angles of attack attained, the pitching-moment data show almost no unstable trends throughout the range of Mach numbers to 0.92. In fact, the only instance of any unstable trend of pitching-moment coefficients occurred at a lift coefficient of 1.0 at a Mach number of 0.80. Reference to figure 9 will show that this unstable trend did not occur with the tail set at more negative incidences. It is probable that the unstable trend of pitching-moment coefficients was caused by decreasing lift-curve slope of the tail or perhaps even stalling of the tail. The use of a tail with a higher stalling angle would probably eliminate all tendency toward longitudinal instability within the range of angles of attack of these tests.

As has been discussed previously, the marked increase in longitudinal stability at the higher lift coefficients indicates that this horizontal tail is larger than it should be to attain minimum change of dC_m/dC_L throughout the angle-of-attack range.

Effects of Flaps

All tests of the model with flaps were made at a Mach number of 0.25 and a Reynolds number of 8,000,000. Lift and pitching-moment data are presented in figure 15 for the model with and without extended split flaps of spans 0.50 b/2 and 0.75 b/2 and with and without an outboard horizontal tail. From these data it was decided that further tests with flaps would be made using the flap having a span of 0.50 b/2 because of the relatively small gain in flap effectiveness and large increase in negative pitching moment for the tail-off condition due to extending the flap to 0.75 b/2. The results of further tests with the large outboard tail in other positions and with the conventional sweptback tail are presented in figure 16. The effects of raising the outboard horizontal tail from $2z/b = 0$ to $2z/b = 0.15$ are indicated to be unfavorable, but lateral displacement of the tail from 0.5 b/2 to 0.4 b/2 caused no adverse effects. Generally, the pitching-moment characteristics with the outboard horizontal tail are as good as or better than those with the conventional tail.

Lift and pitching-moment data for the model with the flap of span 0.50 b/2 are presented in figure 17 for the model with three sizes of outboard tail and with no tail. It is evident that the tail area can be reduced appreciably below that of the large outboard tail while good pitching-moment characteristics are still retained.

In figure 18, the complete lift, drag, and pitching-moment data are presented for the model with a 0.50 b/2 flap, without the outboard tail and with the tail at several angles of incidence. These pitching-moment data were used to compute the downwash parameter $(1 - d\epsilon/d\alpha)$ which, along with the total pitching-moment coefficients and pitching-moment coefficients due to horizontal tail are presented as functions of angle of attack in figure 19. Data were not available for the model with the conventional tail at various angles of incidence and therefore the parameter $(1 - d\epsilon/d\alpha)$ could not be calculated. In general, the flap had no detrimental effects upon the pitching moment due to the horizontal tail for either the outboard tail or the conventional tail (compare figs. 10(a) and 19).

CONCLUSIONS

A horizontal-tail arrangement has been investigated in which the tail surfaces are mounted on booms extending rearward from approximately the mid-semispan of a sweptback wing. The principal objective is to obtain a sweptback wing airplane configuration having static longitudinal stability throughout a large lift range even though the wing itself tends to become unstable over part of the lift range. The airplane arrangement which results seems to offer a number of design advantages which tend to

offset the rather obvious structural disadvantages. Exploratory tests in the Ames 12-foot pressure wind tunnel to a Mach number of 0.92 enable the following conclusions:

1. Outboard horizontal tails, properly positioned, can be a very effective means of counteracting the trend toward longitudinal instability which is characteristic of many sweptback wings at moderate to high lift coefficients. For one configuration tested, undesirable variations in longitudinal stability with lift coefficient were essentially eliminated.

2. Large and favorable changes in the rate of change of downwash with angle of attack occur behind the outer portions of a sweptback wing as the wing develops static longitudinal instability. No theory was found which could reasonably be applied to estimating these downwash changes.

3. The effectiveness of the outboard tail in preventing static longitudinal instability was improved by lowering the tail from 0.15 b/2 to 0 b/2 above the wing chord plane extended, or by moving the tail outboard from 0.4 b/2 to 0.5 b/2, or by moving the tail farther aft.

4. Minor variations in the rate of change of pitching-moment coefficient with lift coefficient, which occurred for some positions of the outboard tail, could be eliminated by the addition of a single fence to the wing. The range of acceptable outboard tail positions can thus be increased by the judicious use of wing fences.

5. For a given position of the outboard tail, the degree of static longitudinal stability at lift coefficients above that for pitch instability of the wing was approximately a linear function of tail size. The degree of stability in this high-lift range relative to that in the low-lift range could be adjusted by changing the tail size. To the extent that these results can be generalized, it may be concluded that for any particular variation of $(dC_m/dC_L)_{\text{tail off}}$ and of $(1 - d\epsilon/d\alpha)$ with angle of attack, there is a tail-volume coefficient that will produce minimum change of $(dC_m/dC_L)_{\text{tail on}}$ with angle of attack.

6. The outboard tails were effective in reducing adverse changes in longitudinal stability of the configuration with an extended split flap.

Ames Aeronautical Laboratory
National Advisory Committee for Aeronautics
Moffett Field, Calif., Apr. 6, 1956

REFERENCES

1. Sutton, Fred B., and Dickson, Jerald K.: The Longitudinal Characteristics at Mach Numbers up to 0.92 of Several Wing-Fuselage-Tail Combinations Having Sweptback Wings with NACA Four-Digit Thickness Distributions. NACA RM A54L08, 1955.

2. Bandettini, Angelo, and Selan, Ralph: The Effects of Horizontal-Tail Height and a Partial-Span Leading-Edge Extension on the Static Longitudinal Stability of a Wing-Fuselage-Tail Combination Having a Sweptback Wing. NACA RM A53J07, 1954.

3. Boltz, Frederick W., and Shibata, Harry H.: Pressure Distribution at Mach Numbers up to 0.90 on a Cambered and Twisted Wing Having 40° of Sweepback and an Aspect Ratio of 10, Including the Effects of Fences. NACA RM A52K20, 1953.

4. Herriot, John G.: Blockage Corrections for Three-Dimensional-Flow Closed-Throat Wind Tunnels, With Considerations of the Effect of Compressibility. NACA Rep. 995, 1950. (Formerly NACA RM A7B28)

5. Sivells, James C., and Salmi, Rachel M.: Jet-Boundary Corrections for Complete and Semispan Swept Wings in Closed Circular Wind Tunnels. NACA TN 2454, 1951.

6. Diederich, Franklin W.: Charts and Tables for Use in Calculations of Downwash of Wings of Arbitrary Plan Form. NACA TN 2353, 1951.

TABLE I.- GEOMETRIC PROPERTIES OF THE MODEL

Wing	
Aspect ratio	6.03
Taper ratio	0.40
Sweepback, deg	45.0
Reference sections (normal to reference sweepline)	
Root	NACA 0014, a = 0.8 (modified) c_{l_i} = 0.4
Tip	NACA 0011, a = 0.8 (modified) c_{l_i} = 0.4
Area (semispan model), sq ft	5.857
Mean aerodynamic chord, ft	1.480
Incidence (measured in the plane of symmetry), deg	3.0
Flaps (20-percent extended from trailing edge)	
Span	0.50 or 0.75 b/2
Deflection (measured relative to the local chord in planes parallel to the stream), deg	30.7
Horizontal tails	
Airfoil (in streamwise direction) NACA 0004-64	
Sweepback of c/2 line, deg	0
Aspect ratio	
Large	4.00
Medium	4.00
Small	3.36
Taper ratio	
Large	0.33
Medium	0.33
Small	0.41
Span (semispan model), ft	
Large	1.868
Medium	1.628
Small	1.176
Area (semispan model), sq ft	
Large	0.872
Medium	0.663
Small	0.412
Tail-volume coefficient	
Large	
At 0.4 b/2	0.346
At 0.5 b/2	0.301 or 0.388
Medium, at 0.5 b/2	0.295
Small, at 0.5 b/2	0.184
Tail heights (measured from the plane of the wing root chord and leading edge) 2z/b	0 or 0.15

TABLE I.- GEOMETRIC PROPERTITIES OF THE MODEL - Concluded

Fuselage

Fineness ratio	12.6
Frontal area, sq ft	0.273

Coordinates:

Distance from nose, in.	Radius, in.
0	0
1.27	1.04
2.54	1.57
5.08	2.35
10.16	3.36
20.31	4.44
30.47	4.90
39.44	5.00
50.00	5.00
60.00	5.00
70.00	5.00
76.00	4.96
82.00	4.83
88.00	4.61
94.00	4.27
100.00	3.77
106.00	3.03
126.00	0

Notes:

(1) Wing sections perpendicular to the sweep axis have NACA 00XX thickness distributions combined with an NACA $a = 0.8$ (modified) mean line, $c_{l_i} = 0.4$.

(2) Horizontal tail sections have NACA 0004-64 thickness distributions parallel to the stream.

(3) All dimensions are in inches.

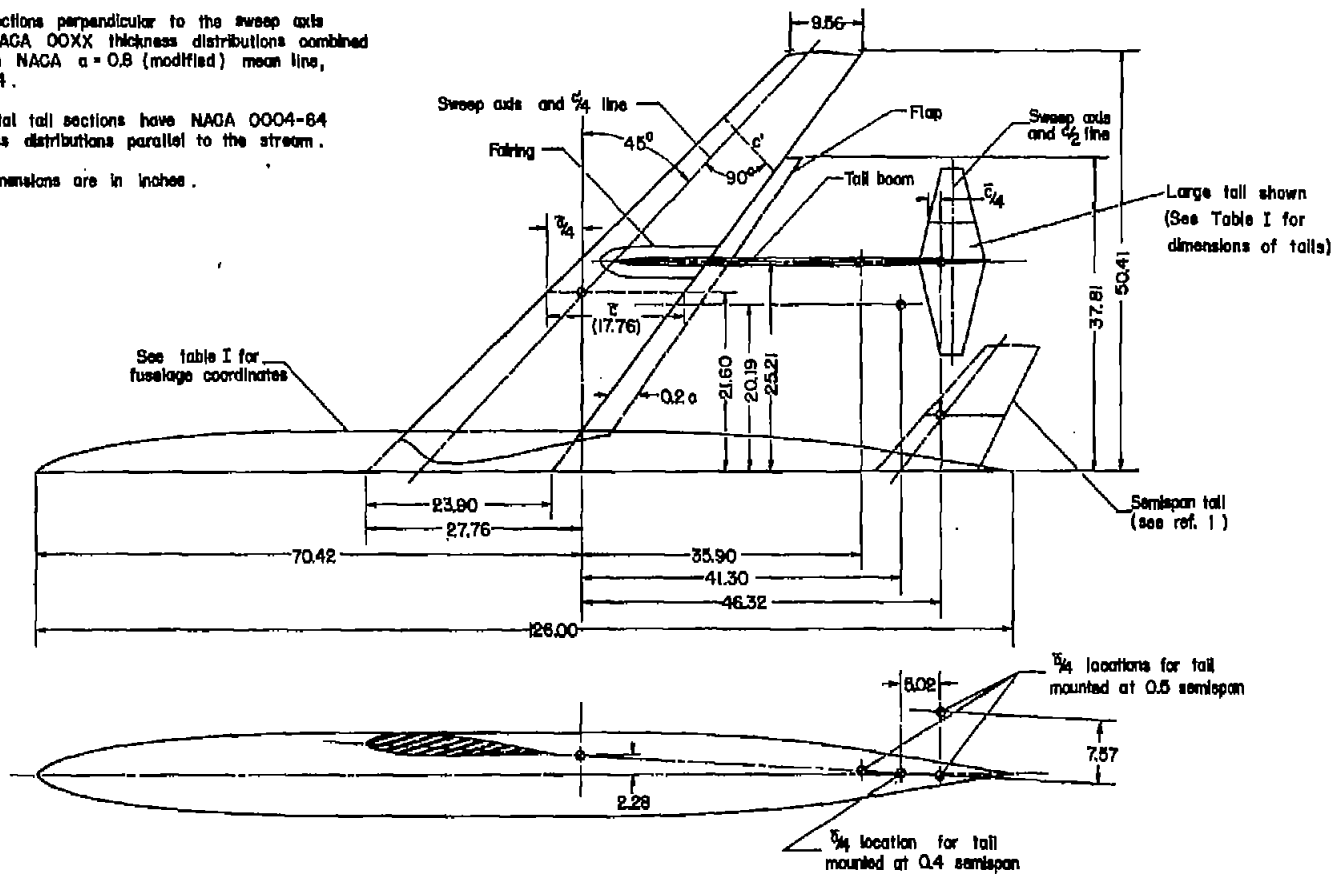

(a) Dimensions.

Figure 1.- Geometry of the model.

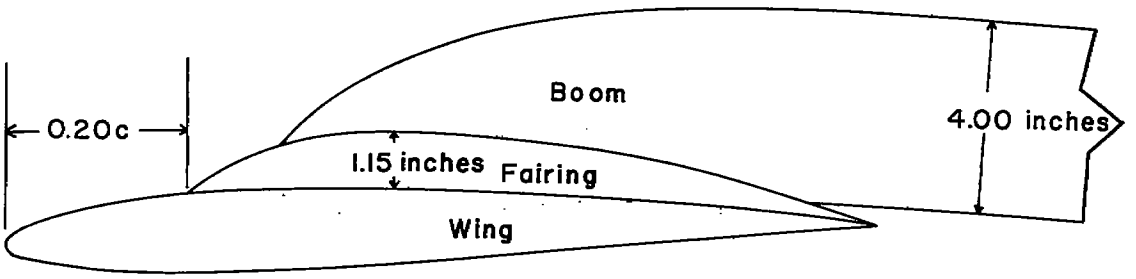

Wing-boom juncture

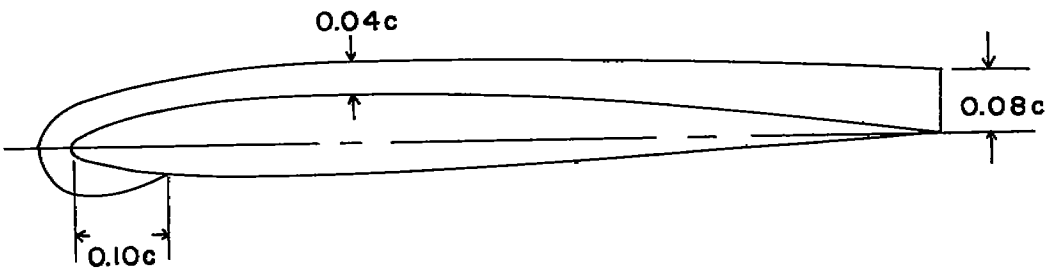

Fence of the present investigation

Fence of the comparative data from reference 1

(b) Wing-boom juncture and wing-fence details.

Figure 1.- Continued.

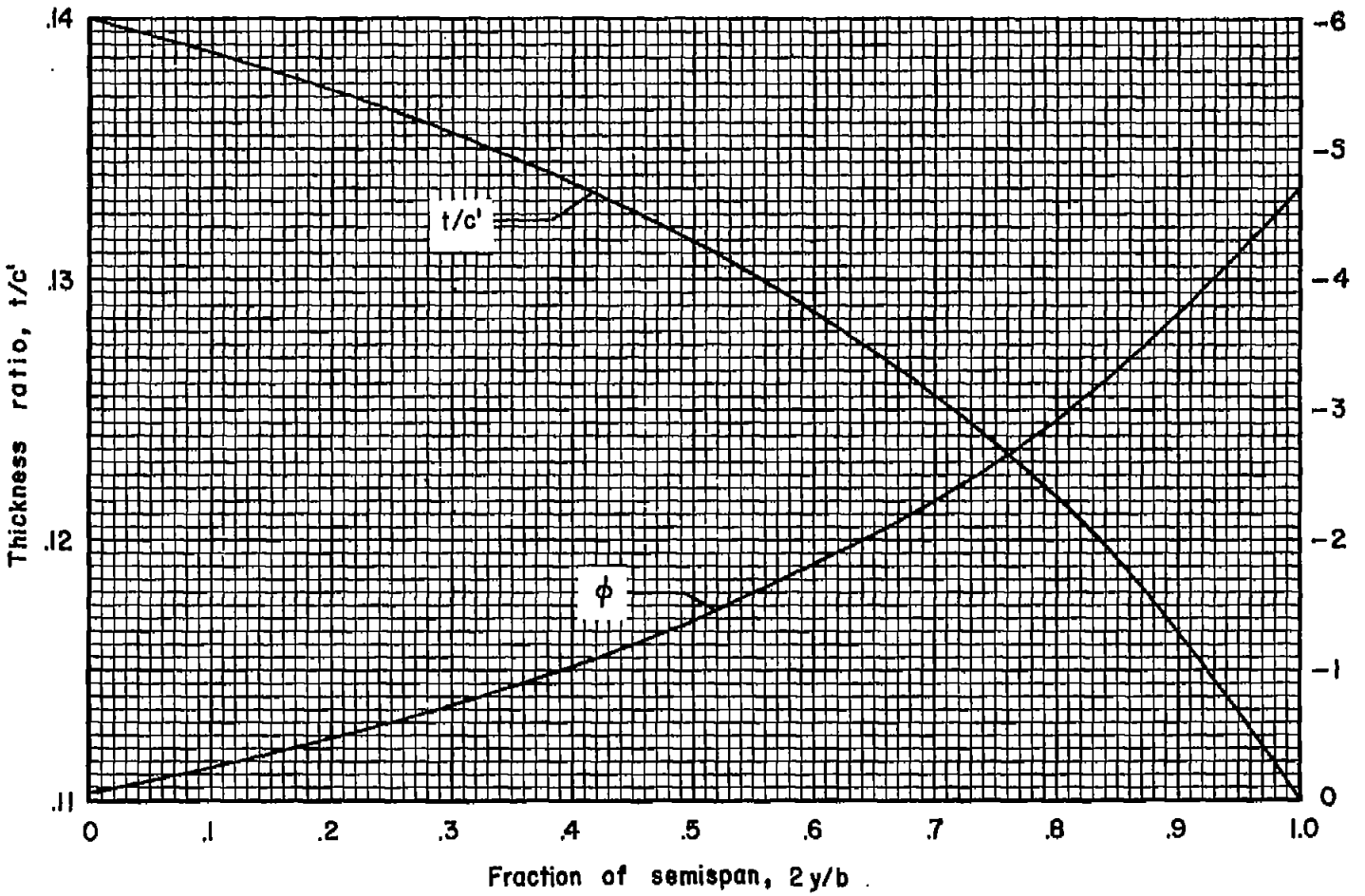

(c) Wing twist and thickness-chord ratio.

Figure 1.- Concluded.

A-20803

A-20787

Figure 2.- Photographs of the model in the wind tunnel.

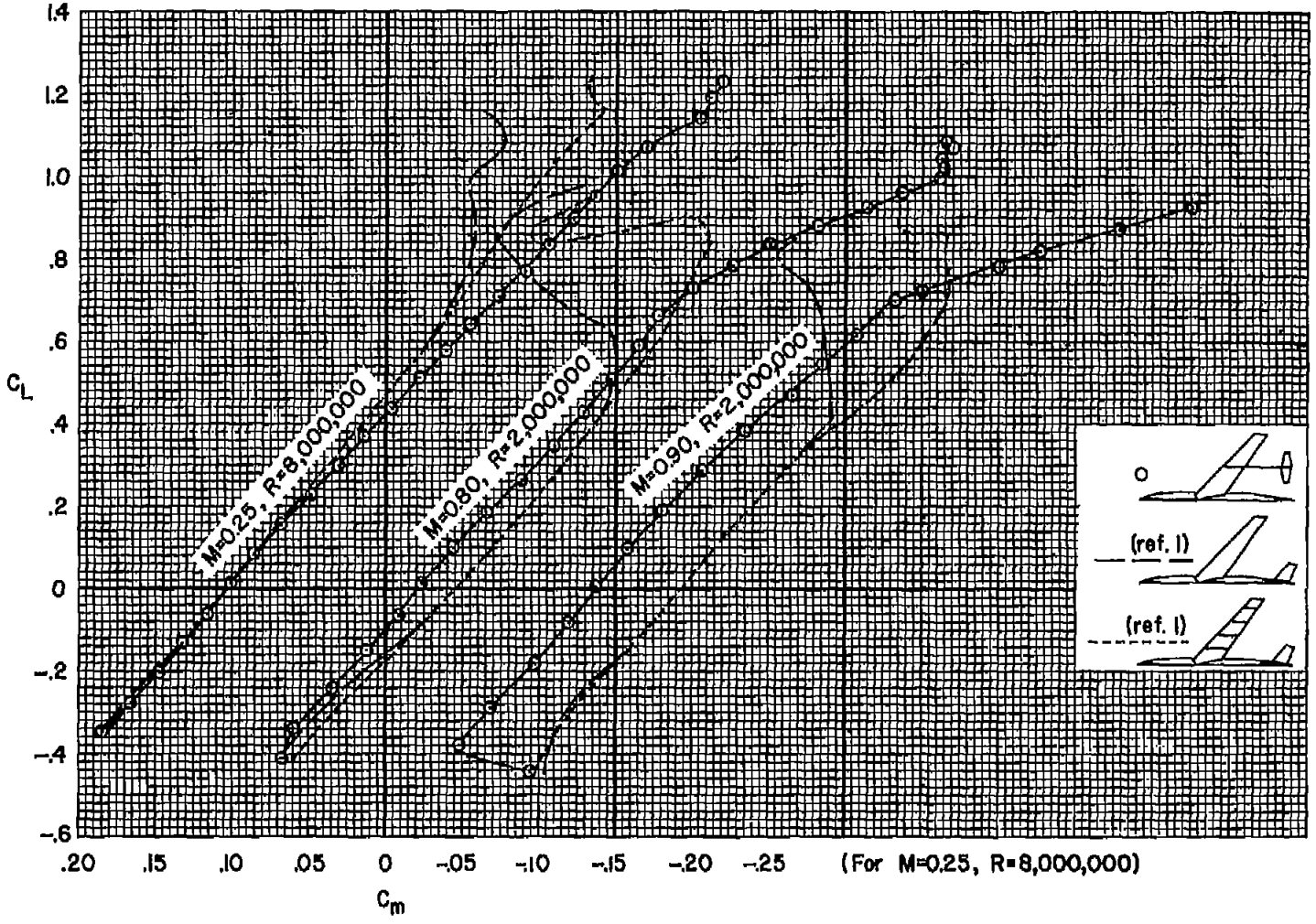

Figure 3.- A comparison of the pitching-moment characteristics of the model with a conventional sweptback tail and with the large outboard tail in the low position at 0.5 b/2; $i_t = -6°$.

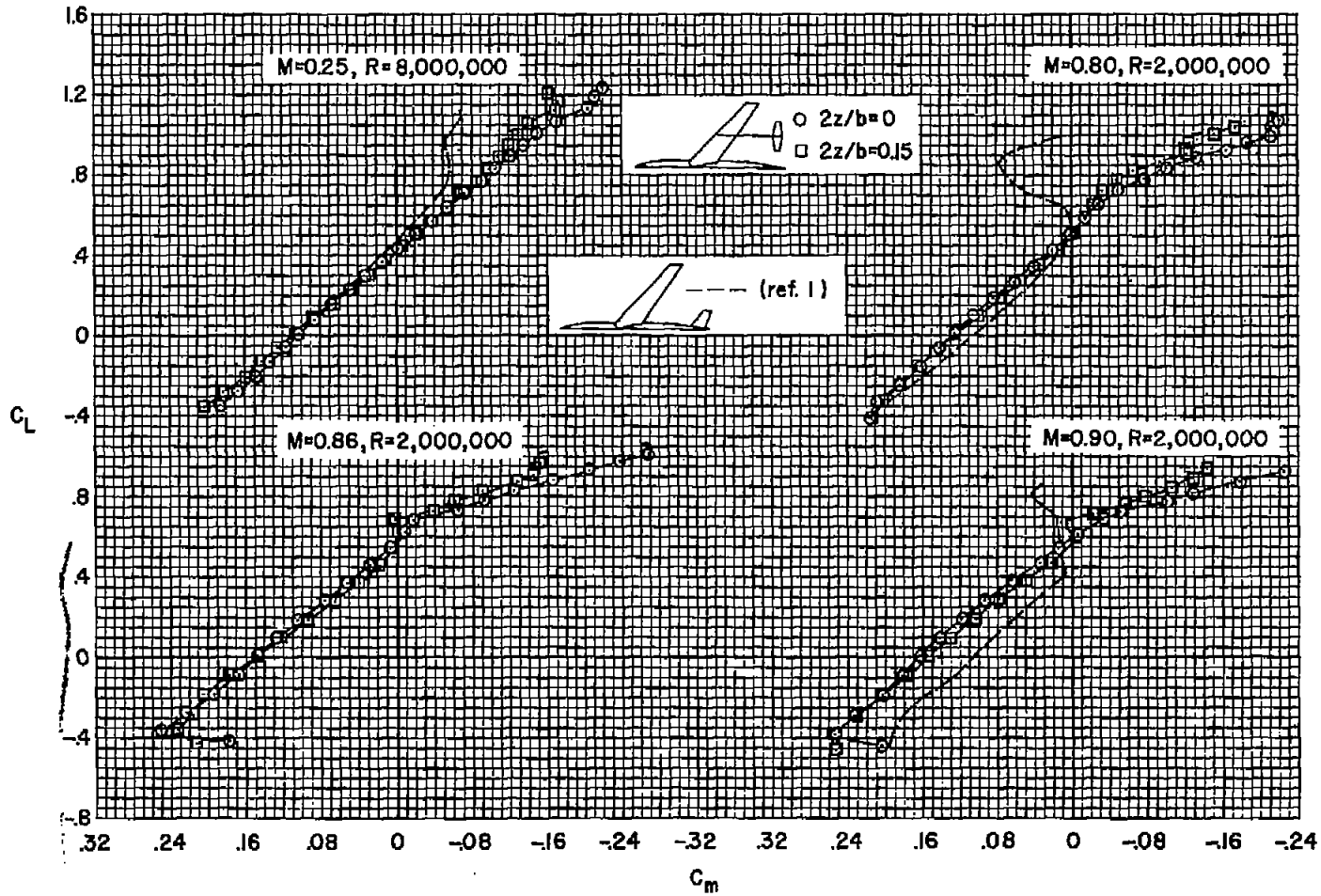

(a) Effects of changing vertical position of horizontal tail.

Figure 4.- The effects of changes in horizontal-tail position on the pitching-moment characteristics of the model; $i_t = -6^\circ$.

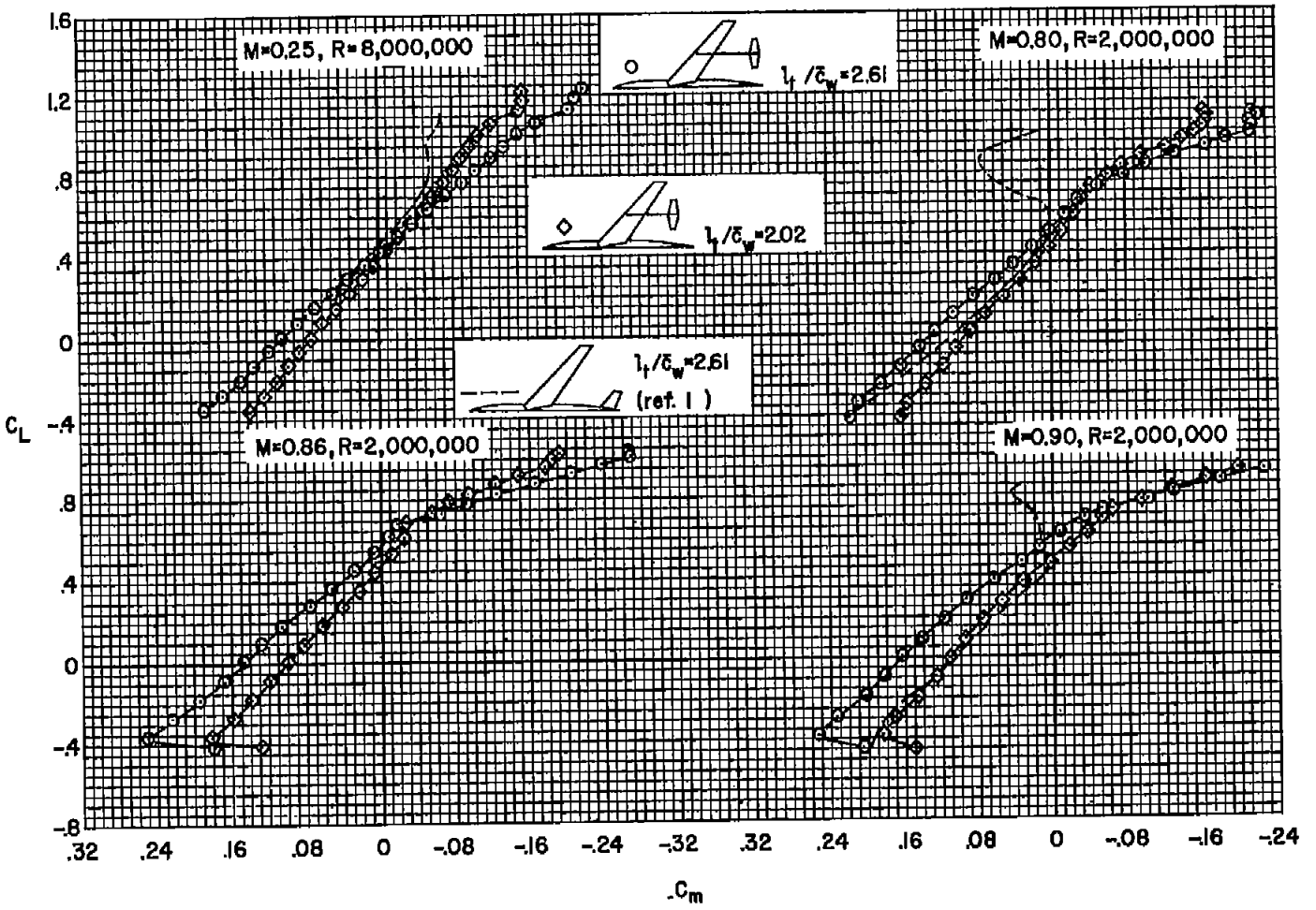

(b) Effects of changing longitudinal position of horizontal tail.

Figure 4.- Continued.

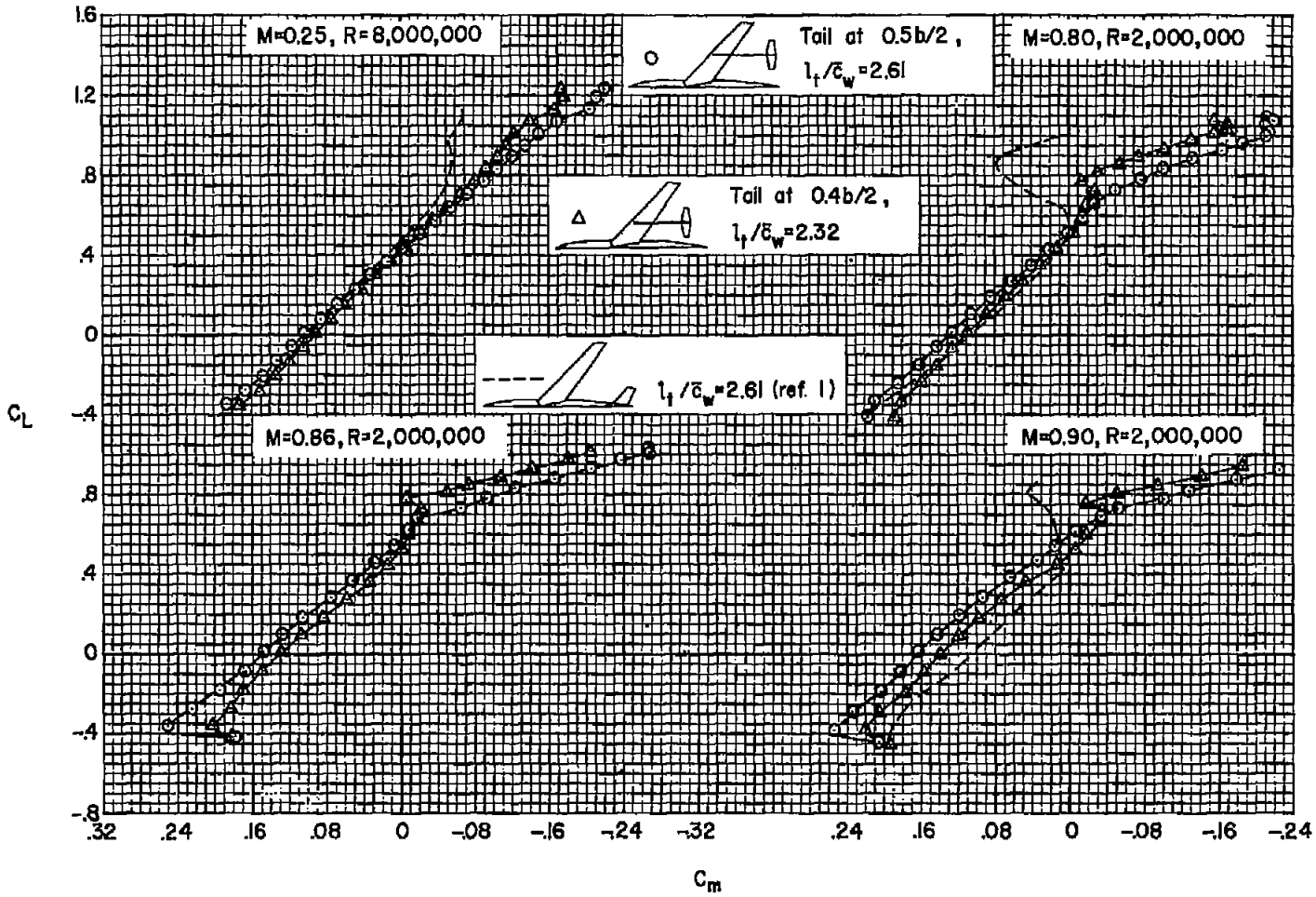

(c) Effects of changing lateral position of horizontal tail.

Figure 4.- Concluded.

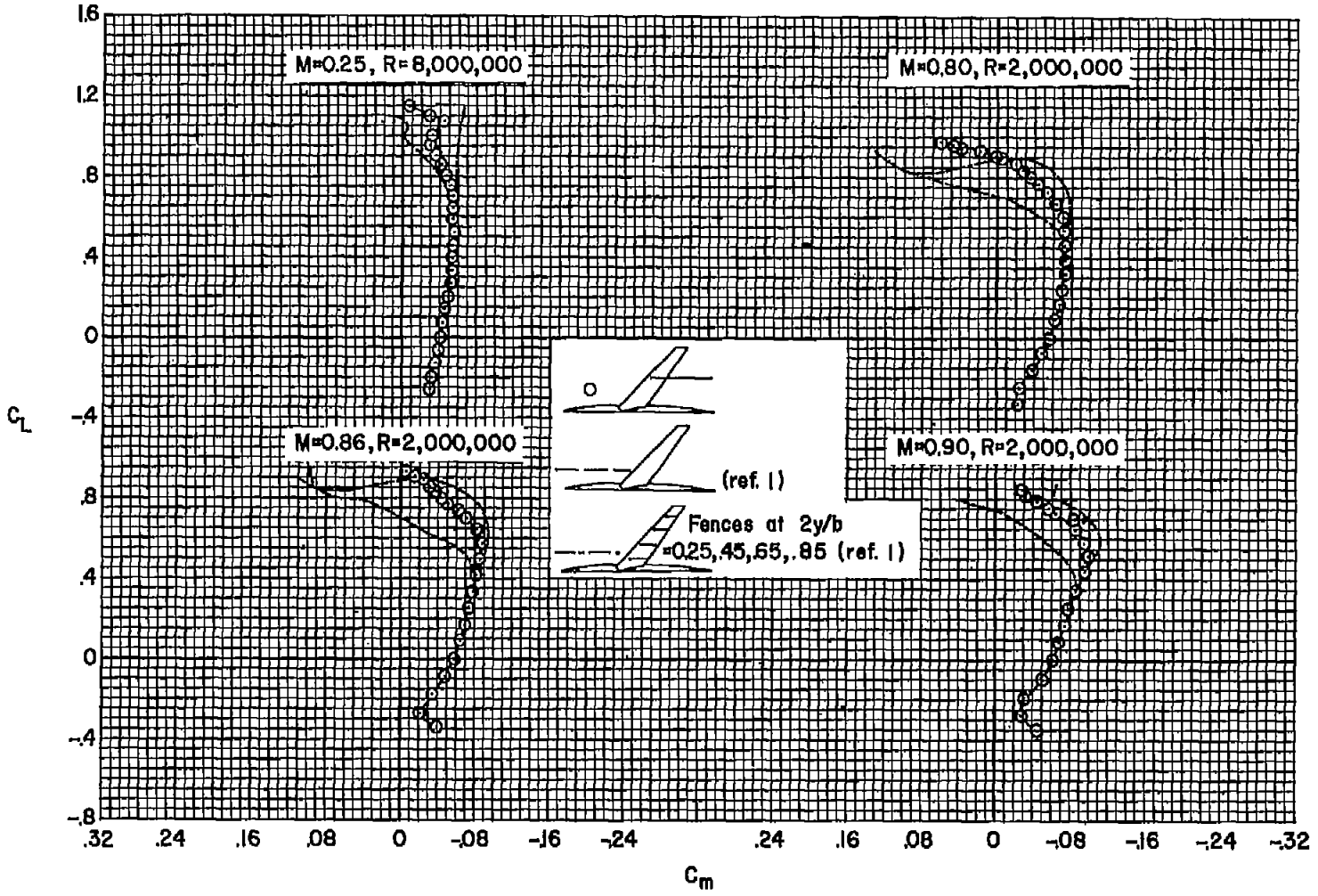

Figure 5.- The effectiveness of the tail-boom as a wing fence.

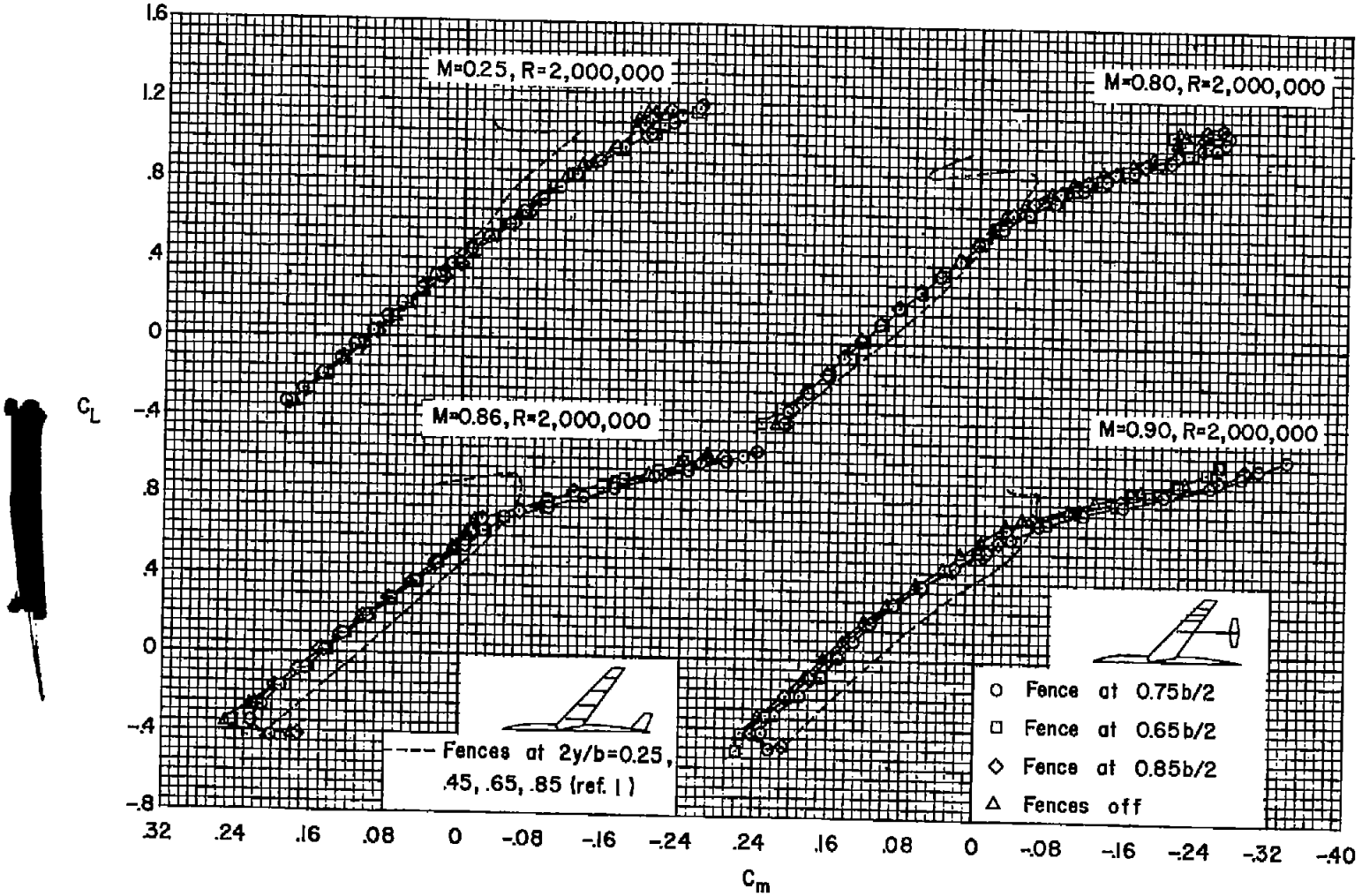

Figure 6.- The effects of a wing fence on the pitching-moment characteristics of the model with the large outboard tail in the low position at 0.5 b/2; $i_t = -6^\circ$.

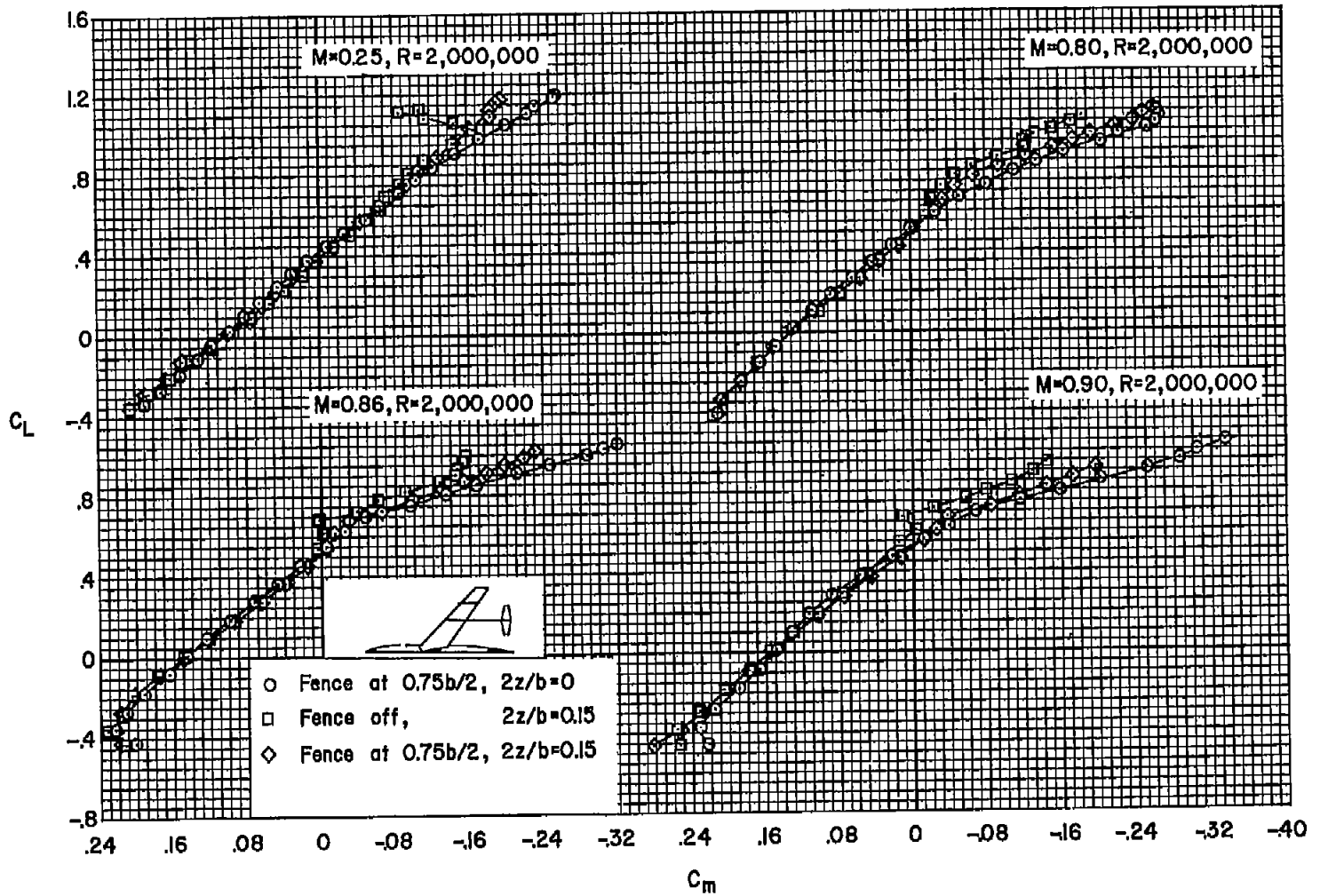

Figure 7.- A comparison of the effects of wing fences on the pitching-moment characteristics of the model for two heights of the large outboard tail at 0.5 b/2; $i_t = -6^\circ$.

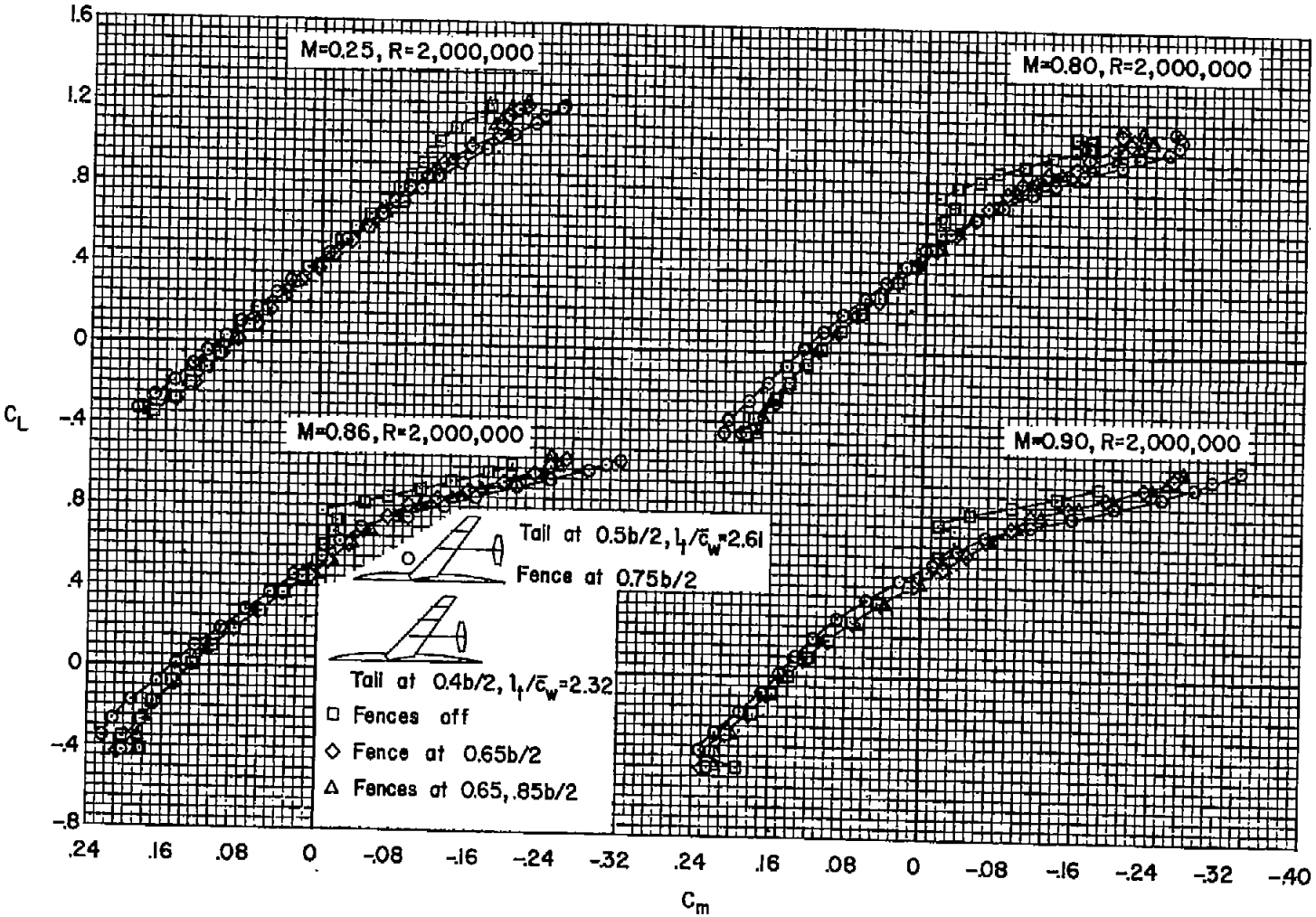

Figure 8.- A comparison of the effects of wing fences on the pitching-moment characteristics of the model for two lateral positions of the large outboard tail; $i_t = -6^\circ$.

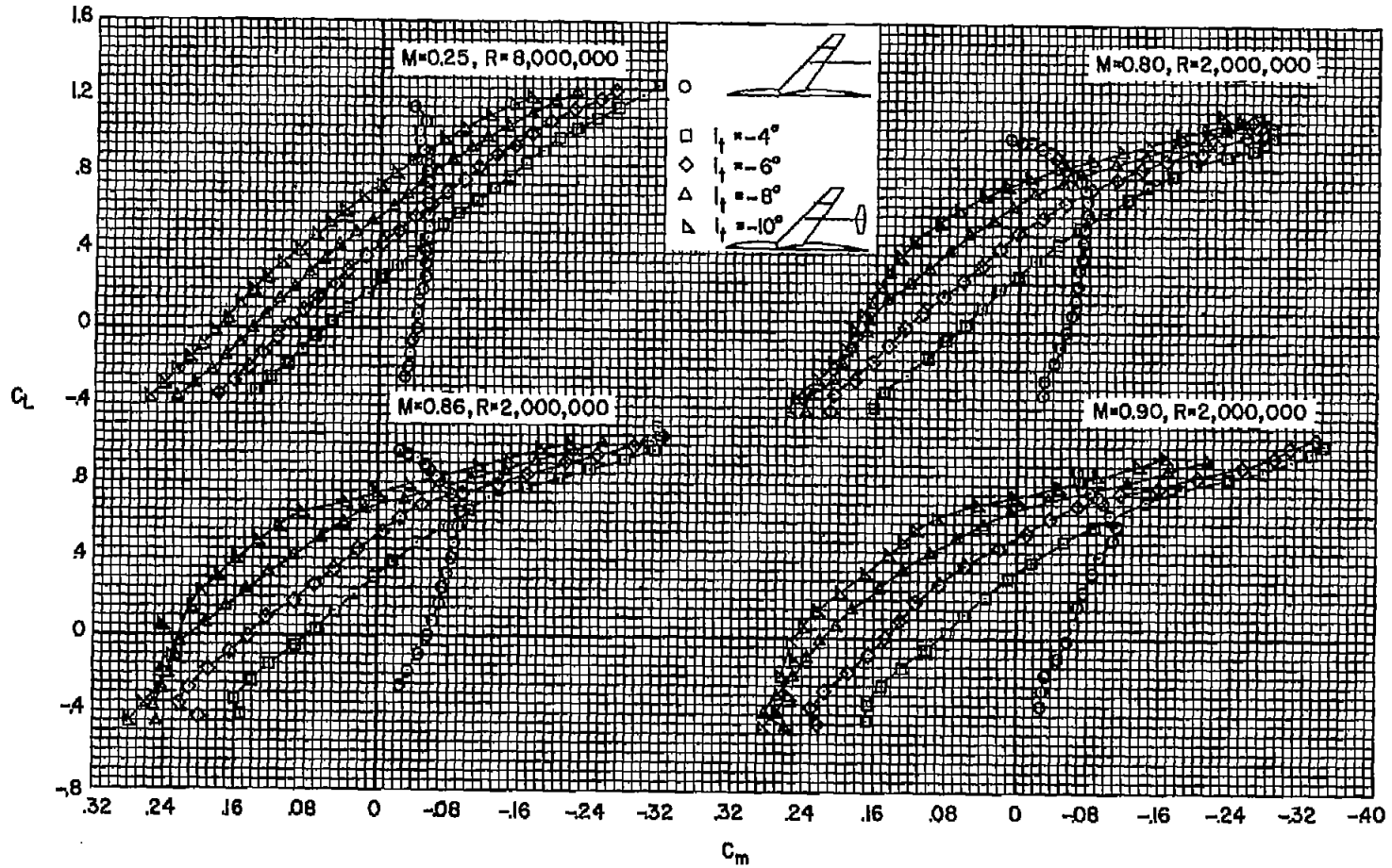

Figure 9.- The pitching-moment characteristics of the model with the large outboard tail at several incidences; tail in low position at 0.5 b/2.

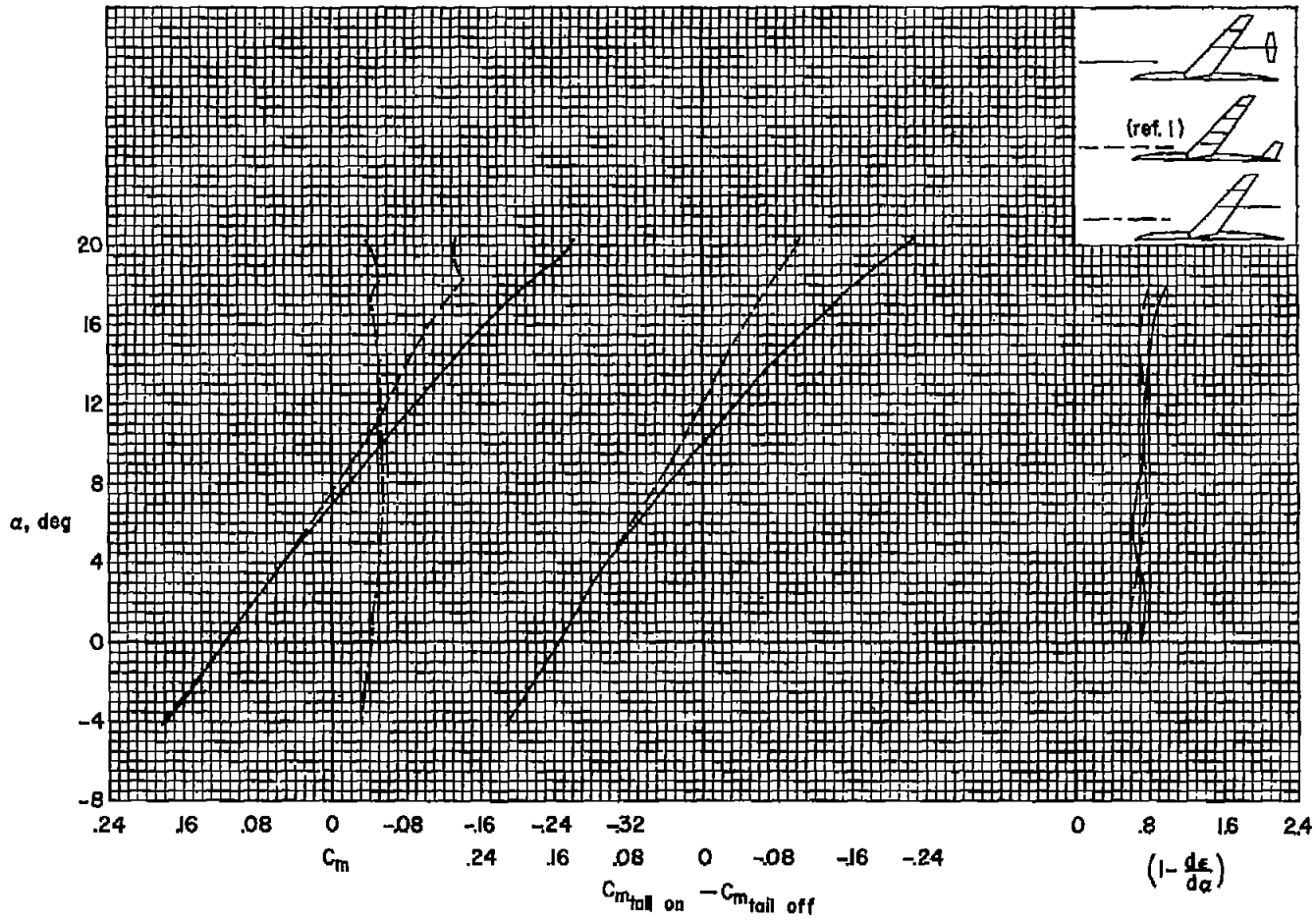

(a) M = 0.25, R = 8,000,000

Figure 10.- A comparison of the variations with angle of attack of total pitching-moment coefficient, pitching-moment coefficient due to horizontal tail, and downwash parameter for the model with the large outboard tail in low position at 0.5 b/2 and with a conventional swept-back tail; $i_t = -6°$.

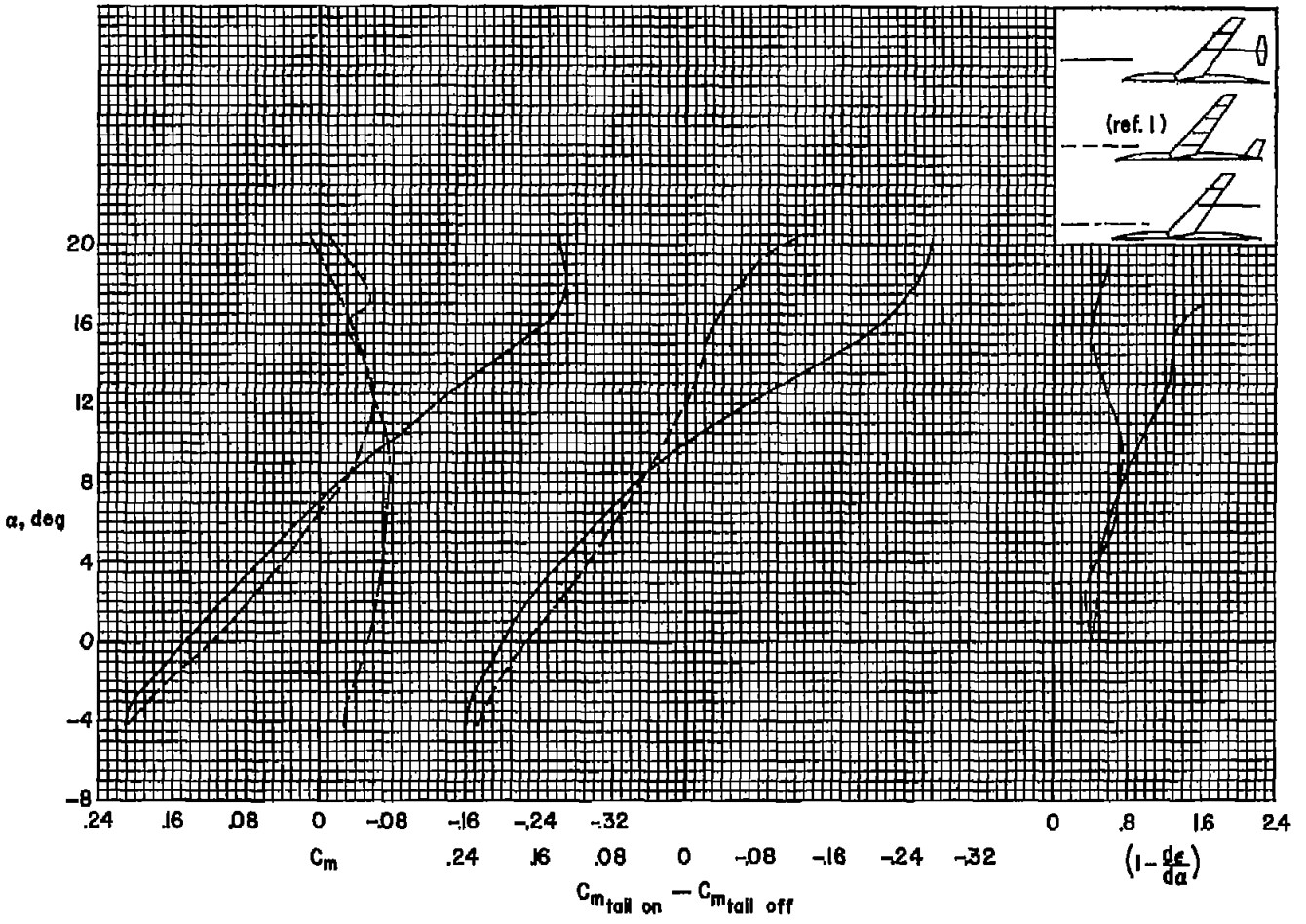

(b) M = 0.80, R = 2,000,000

Figure 10.- Continued.

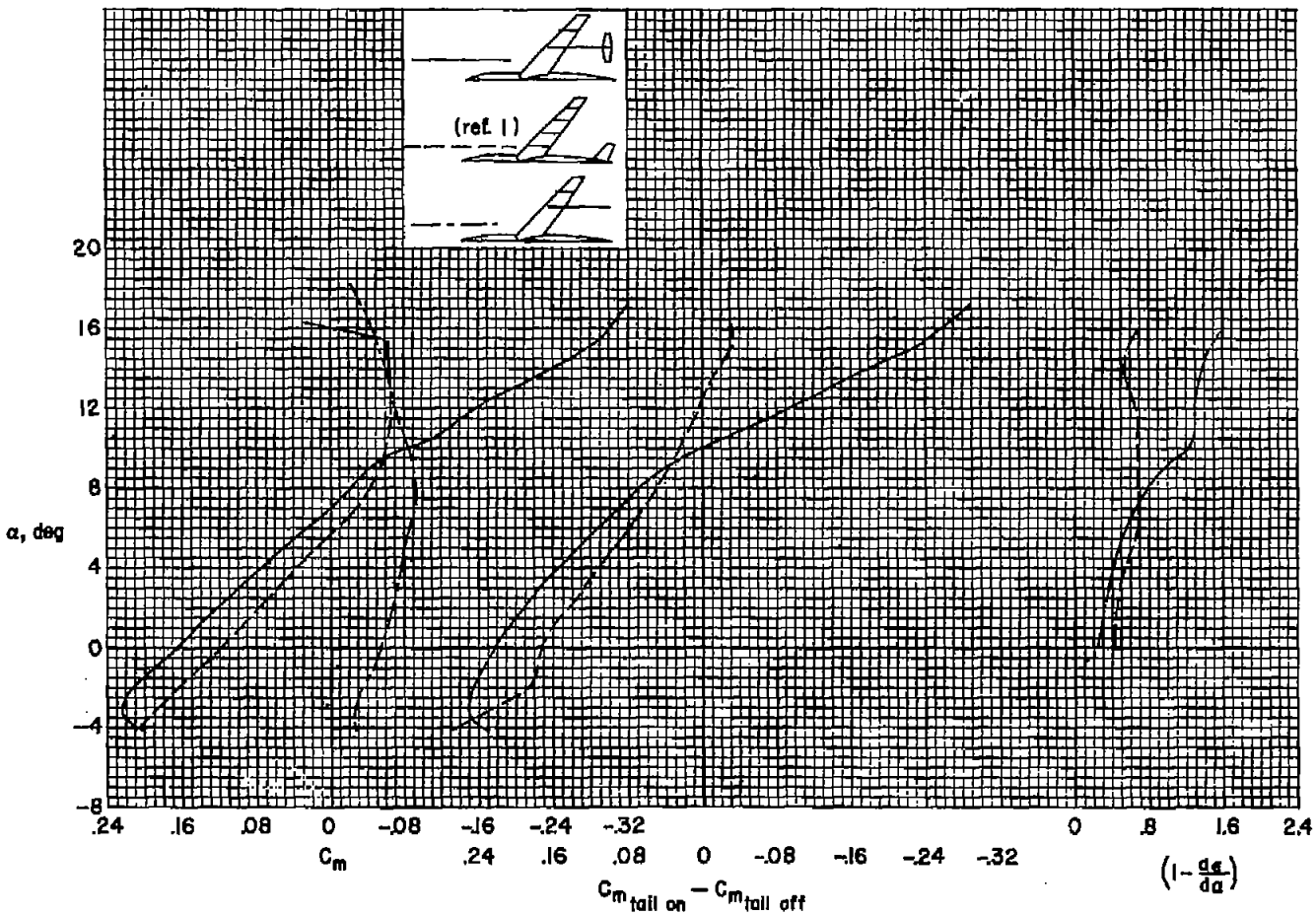

(c) M = 0.86, R = 2,000,000

Figure 10.- Continued.

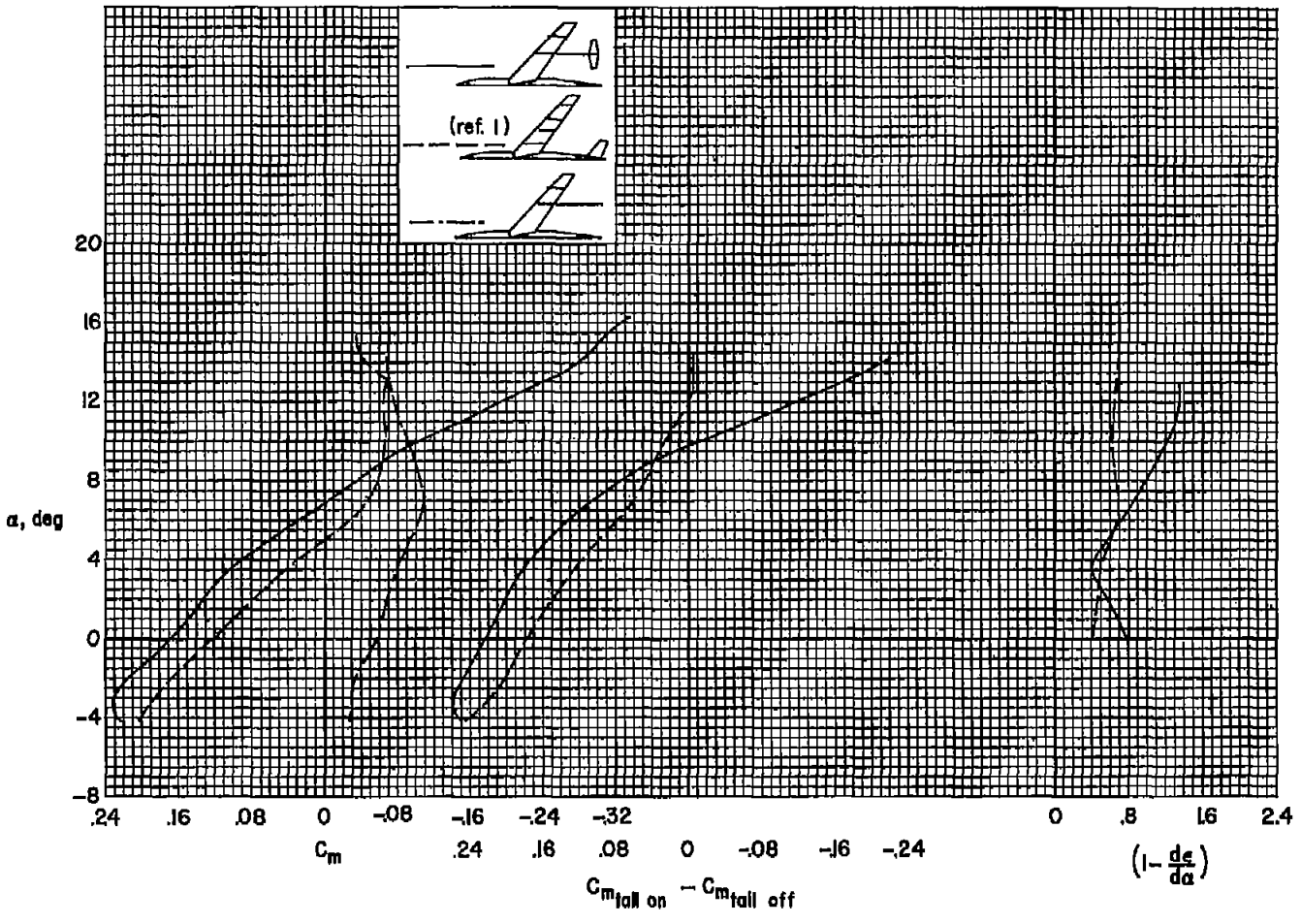

(d) M = 0.90, R = 2,000,000

Figure 10.- Concluded.

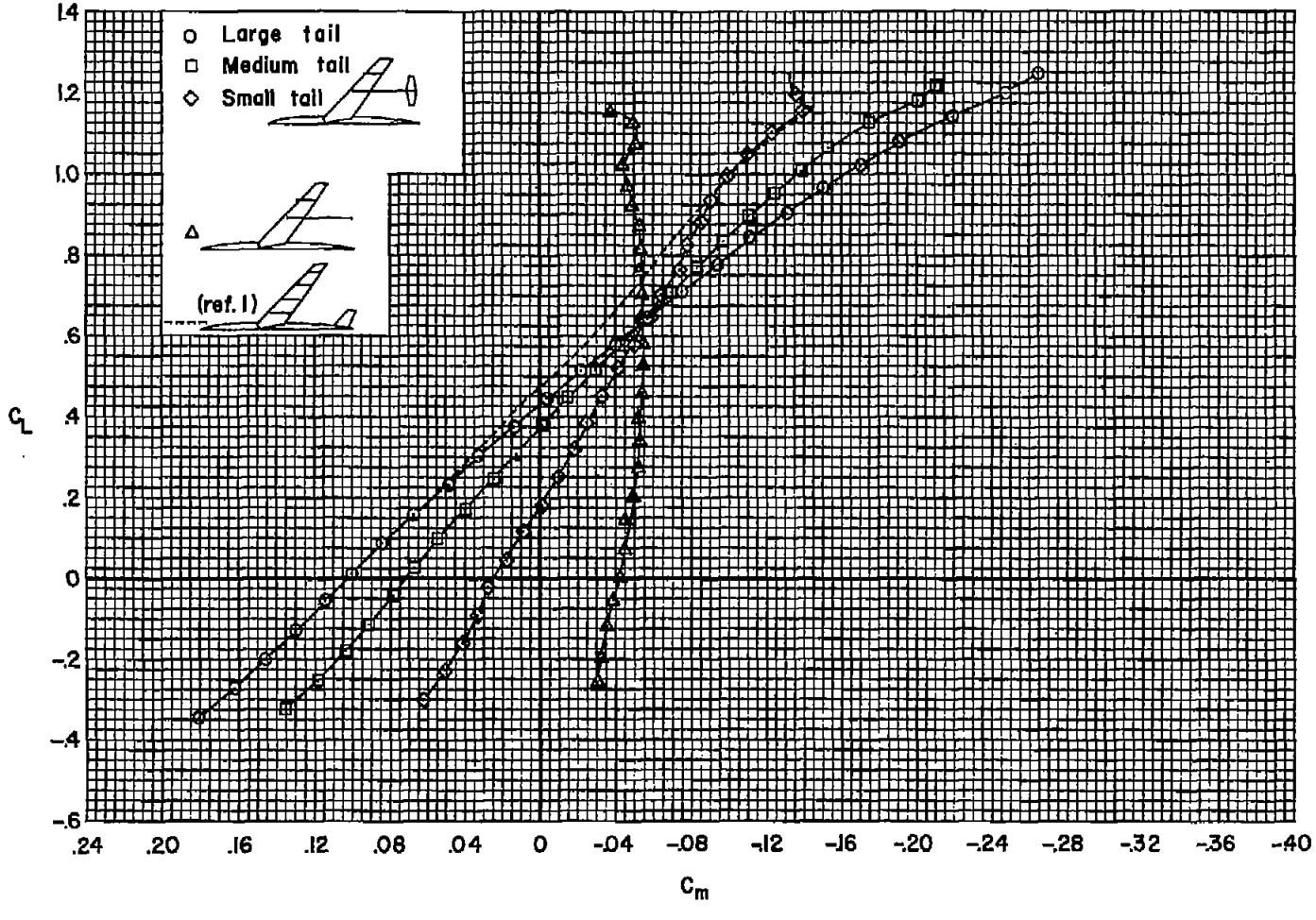

(a) M = 0.25, R = 8,000,000

Figure 11.- The effects of tail size on the pitching-moment characteristics of the model; tails in low position at 0.5 b/2; $i_t = -6°$.

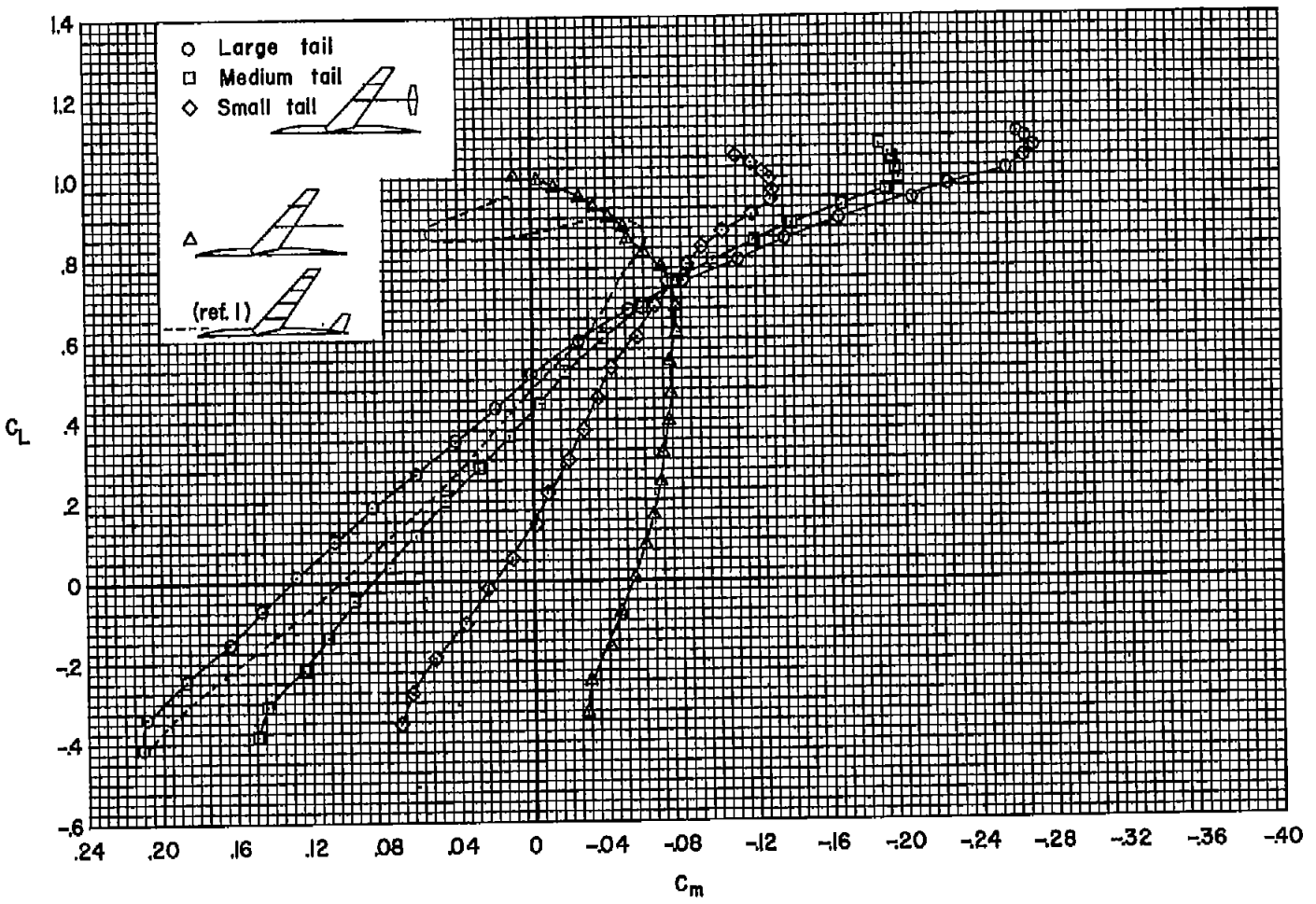

(b) M = 0.80, R = 2,000,000

Figure 11.- Continued.

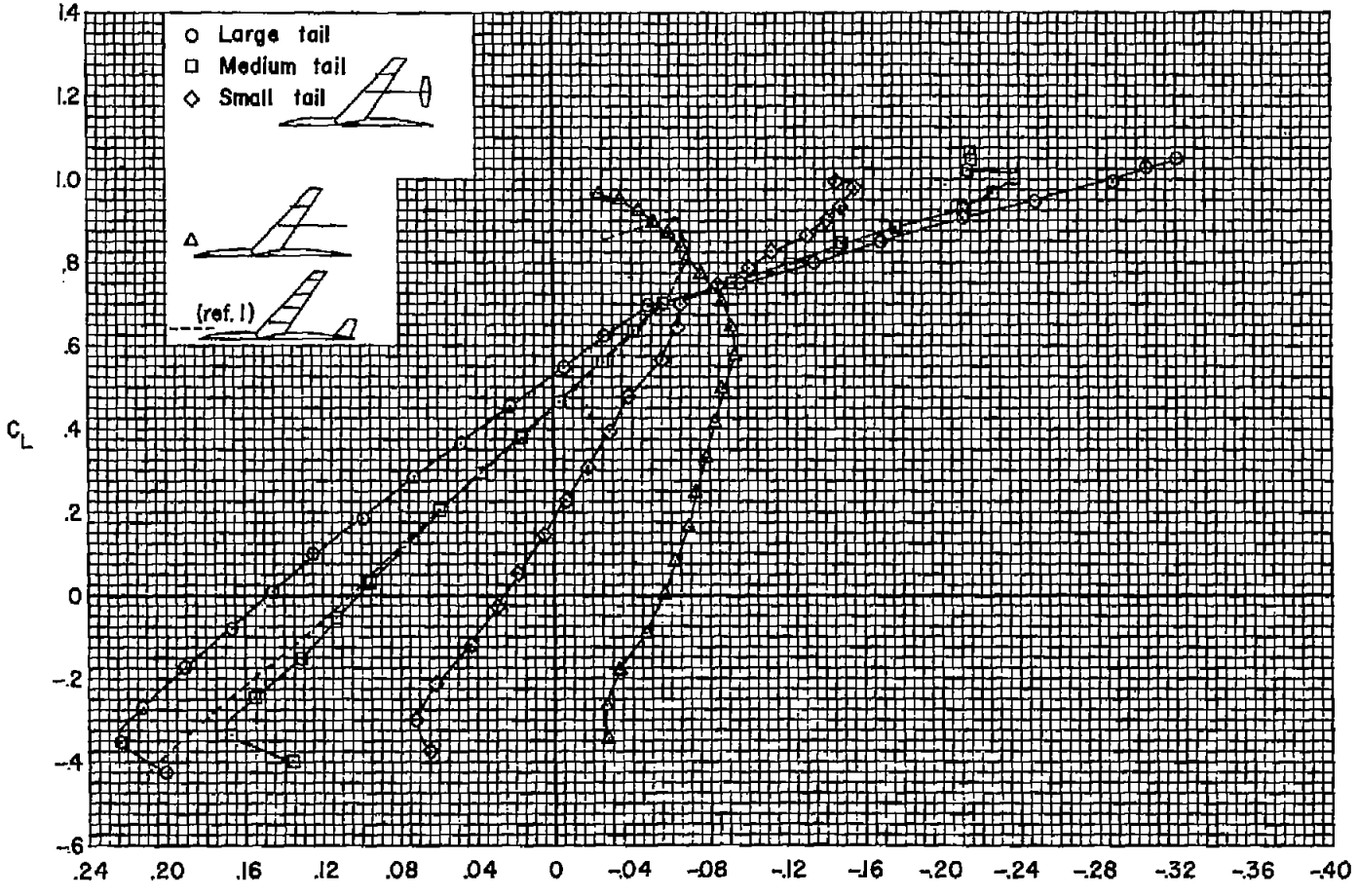

(c) M = 0.86, R = 2,000,000

Figure 11.- Continued.

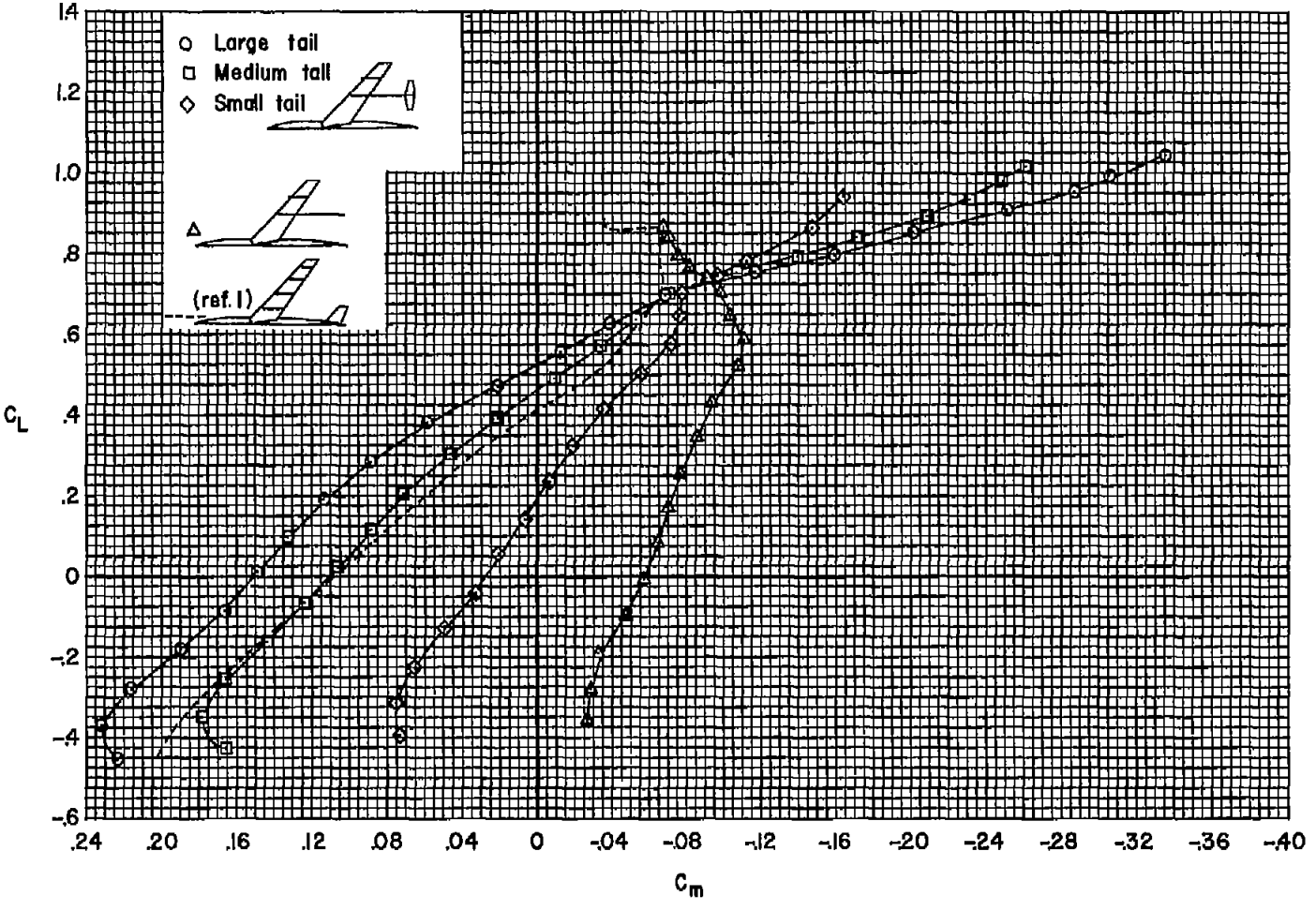

(d) M = 0.90, R = 2,000,000

Figure 11.- Concluded.

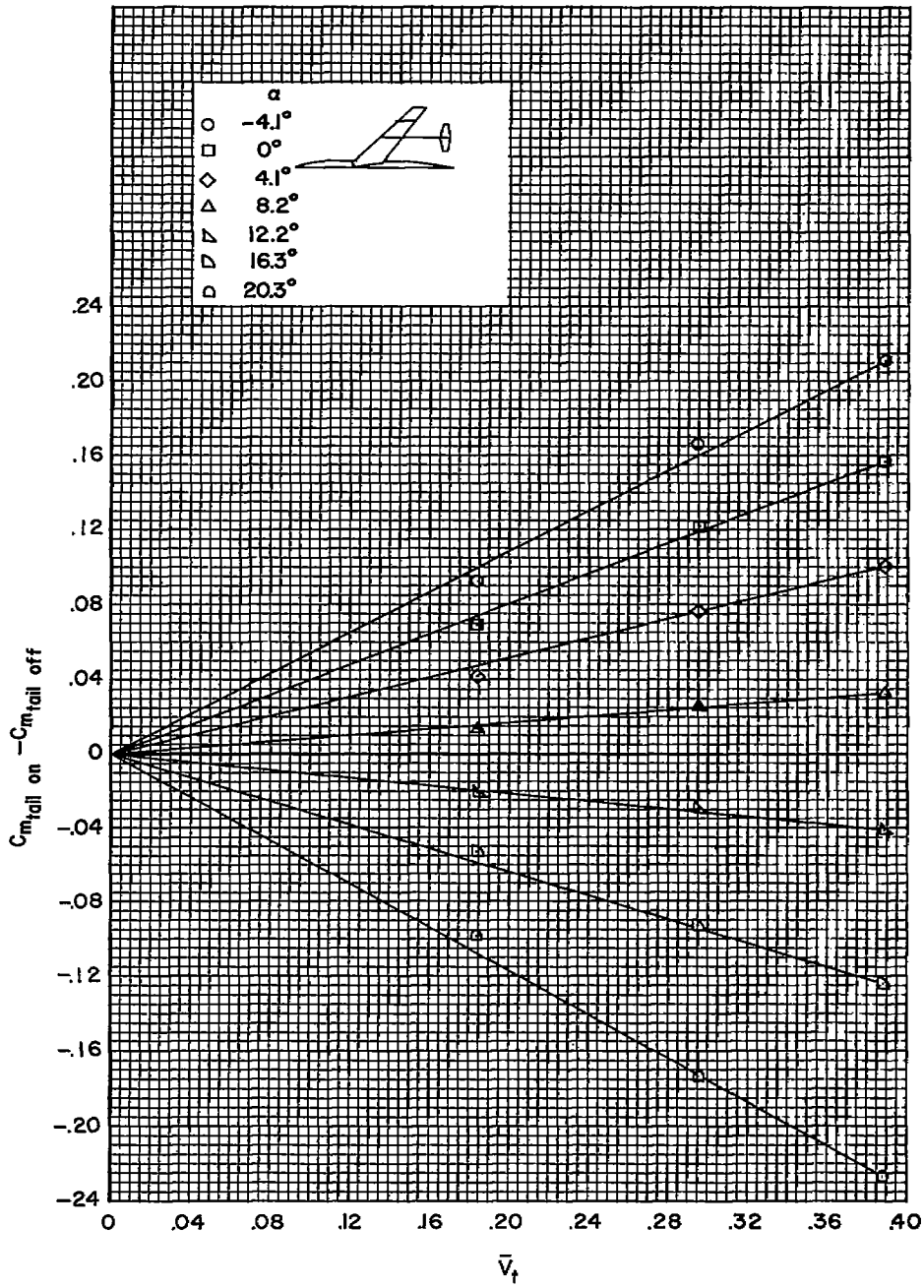

(a) M = 0.25, R = 8,000,000

Figure 12.- The variation of pitching-moment coefficient due to horizontal tail as a function of tail-volume coefficient; tails in low position at 0.5 b/2; $i_t = -6°$.

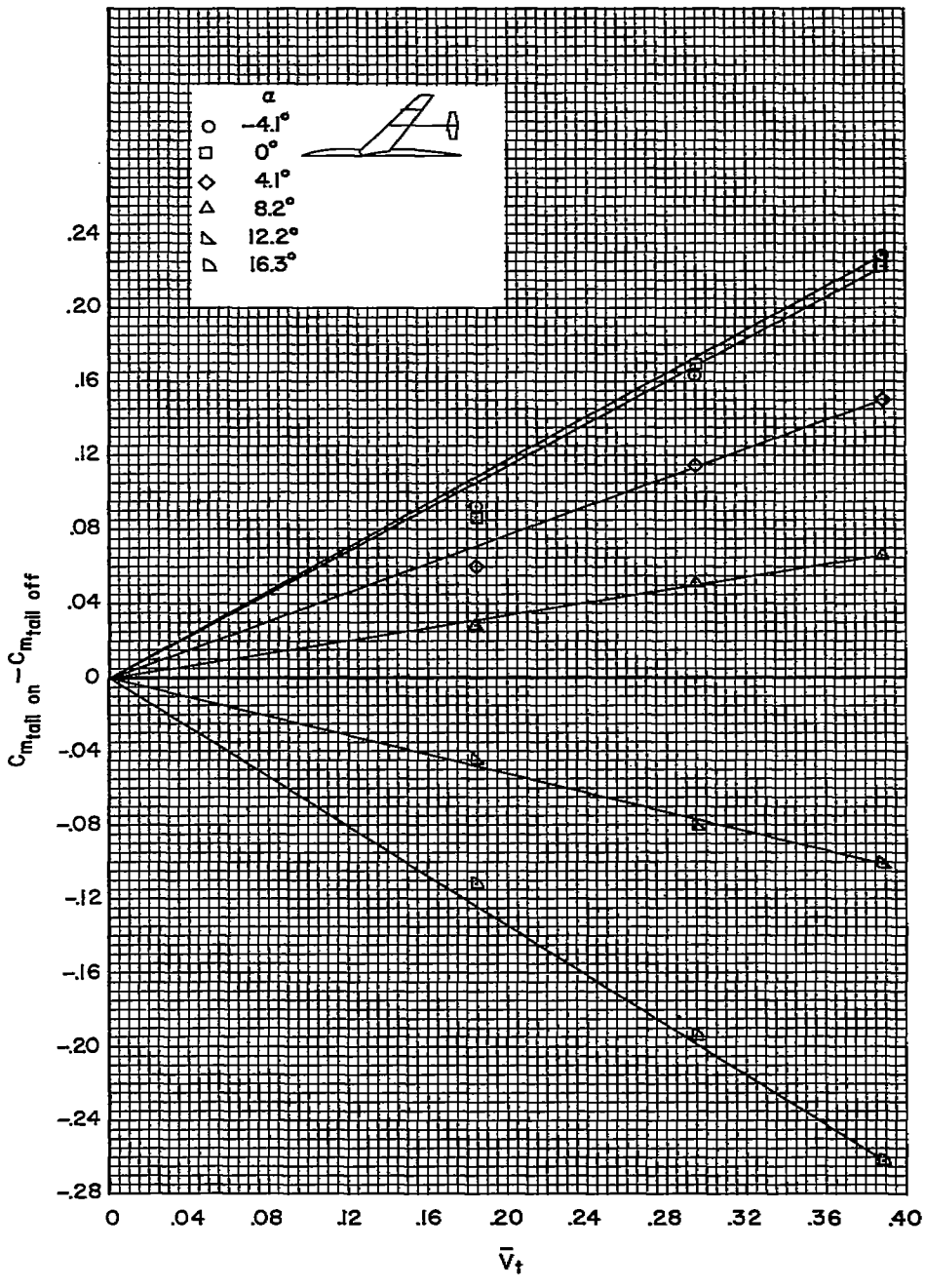

(b) M = 0.86, R = 2,000,000

Figure 12.- Concluded.

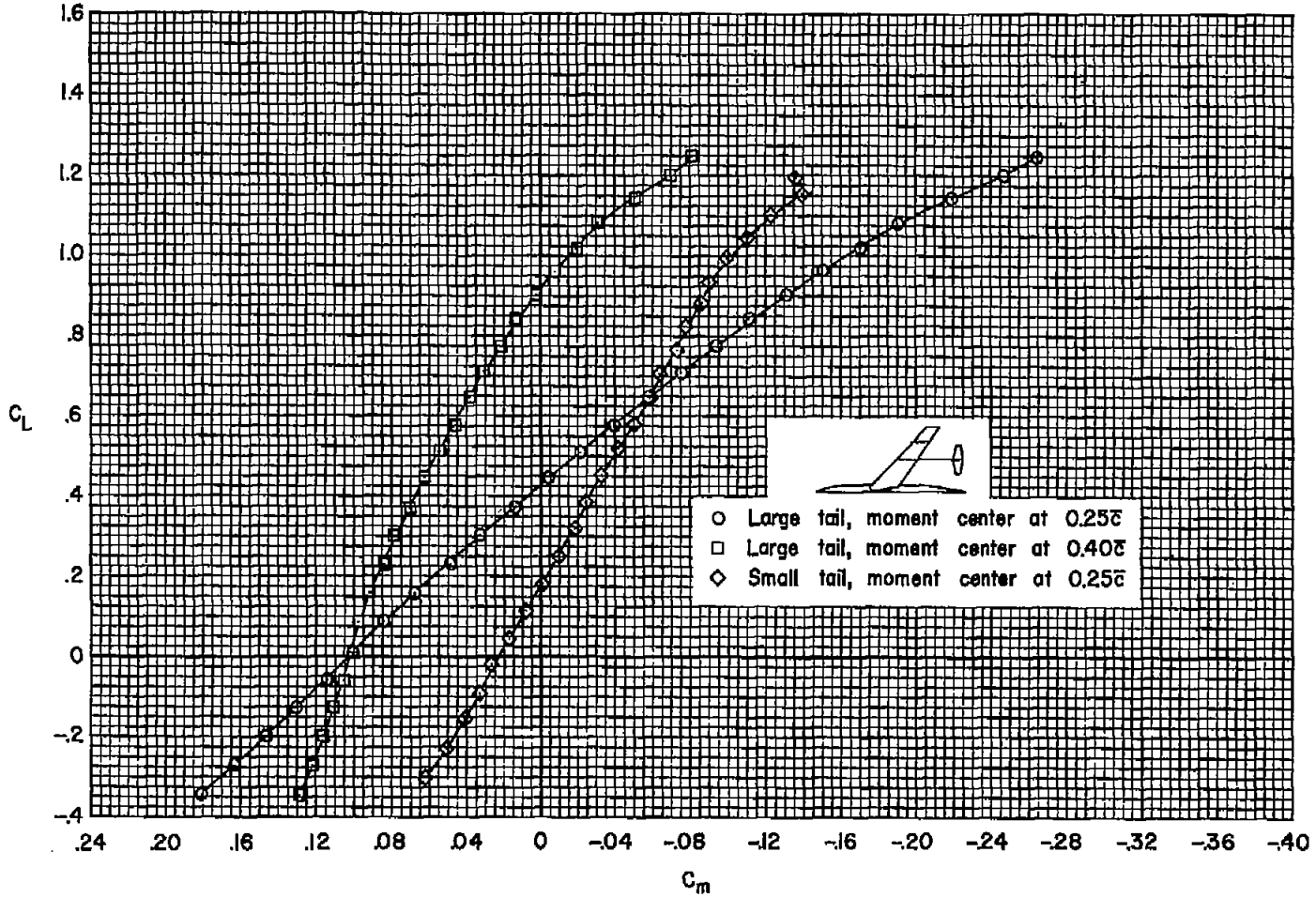

(a) M = 0.25, R = 8,000,000

Figure 13.- A comparison of the changes in pitching-moment characteristics resulting from rearward movement of the moment center and from a reduction of tail size; tails at 0.5 b/2; $i_t = -6^\circ$.

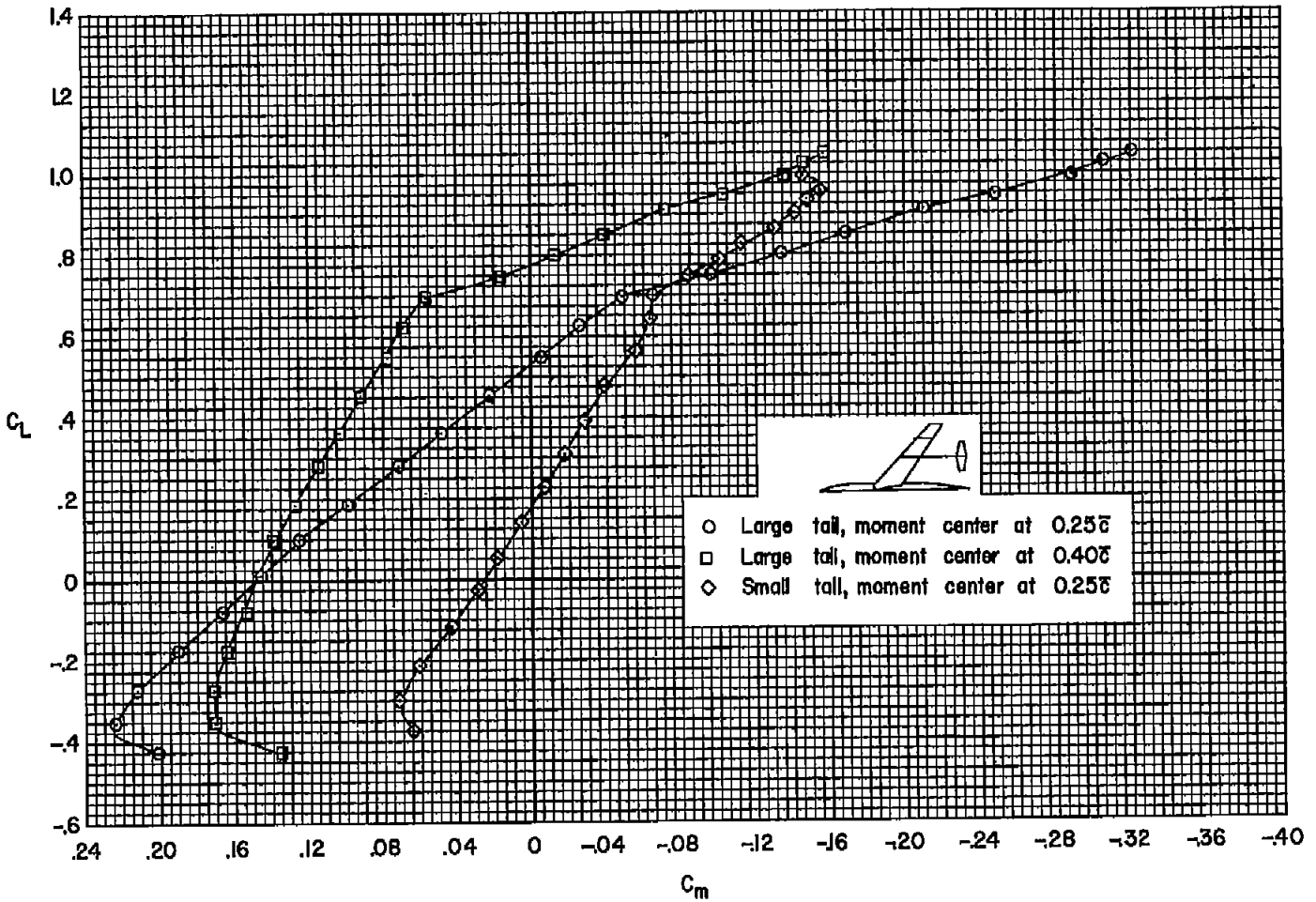

(b) M = 0.86, R = 2,000,000

Figure 13.- Concluded.

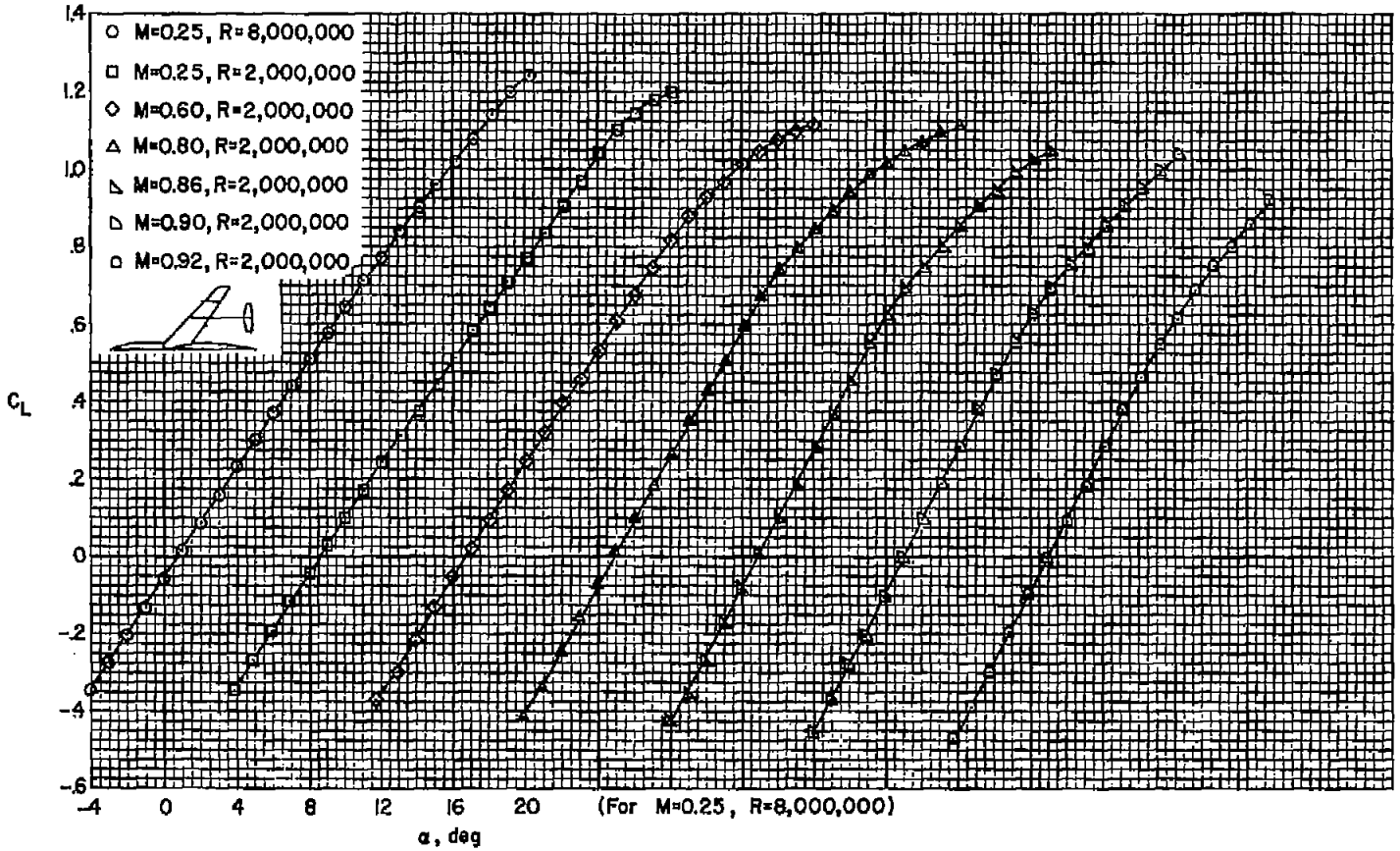

(a) C_L vs. α

Figure 14.- The effects of Mach number on the lift, drag, and pitching-moment characteristics of the model with the large outboard tail mounted in low position at 0.5 b/2; $i_t = -6^\circ$.

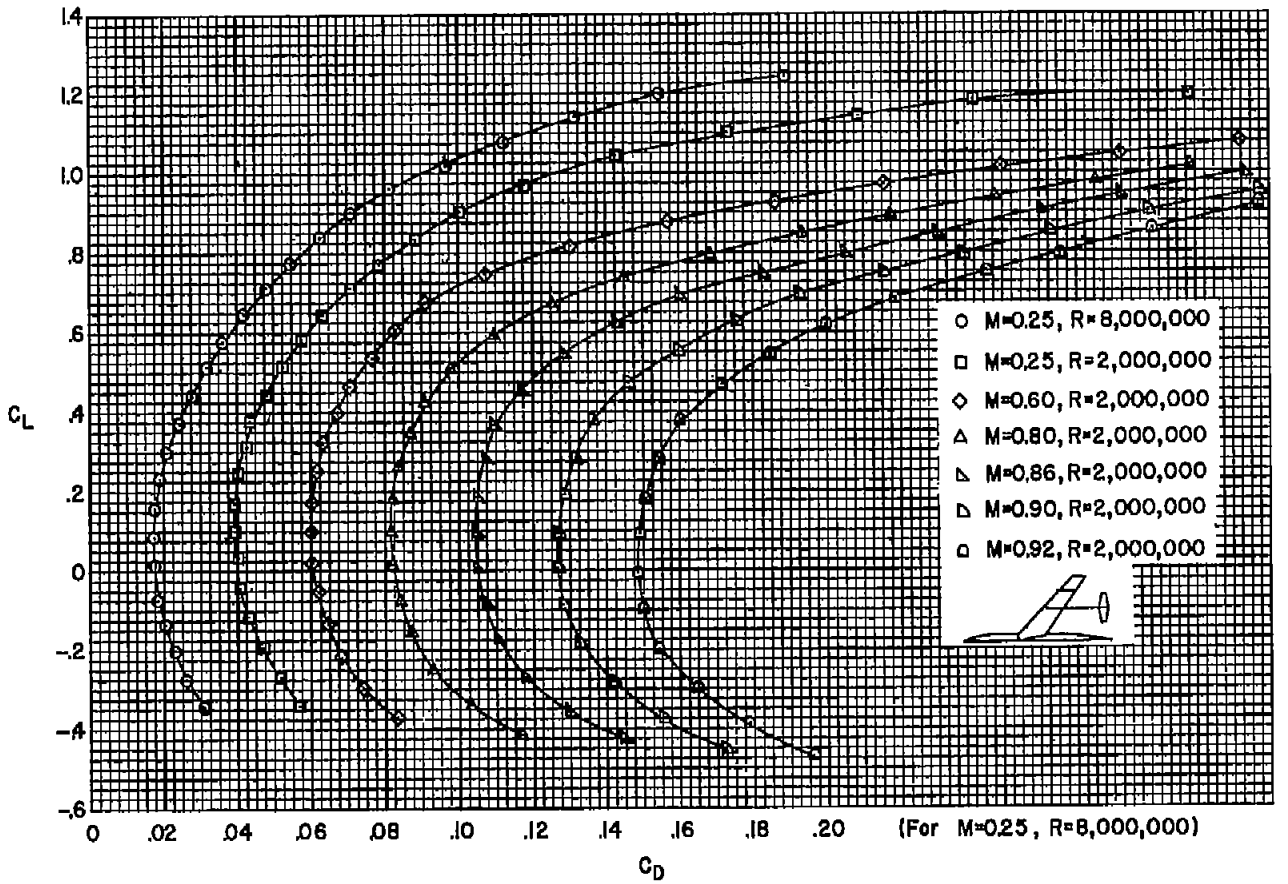

(b) C_L vs. C_D

Figure 14.- Continued.

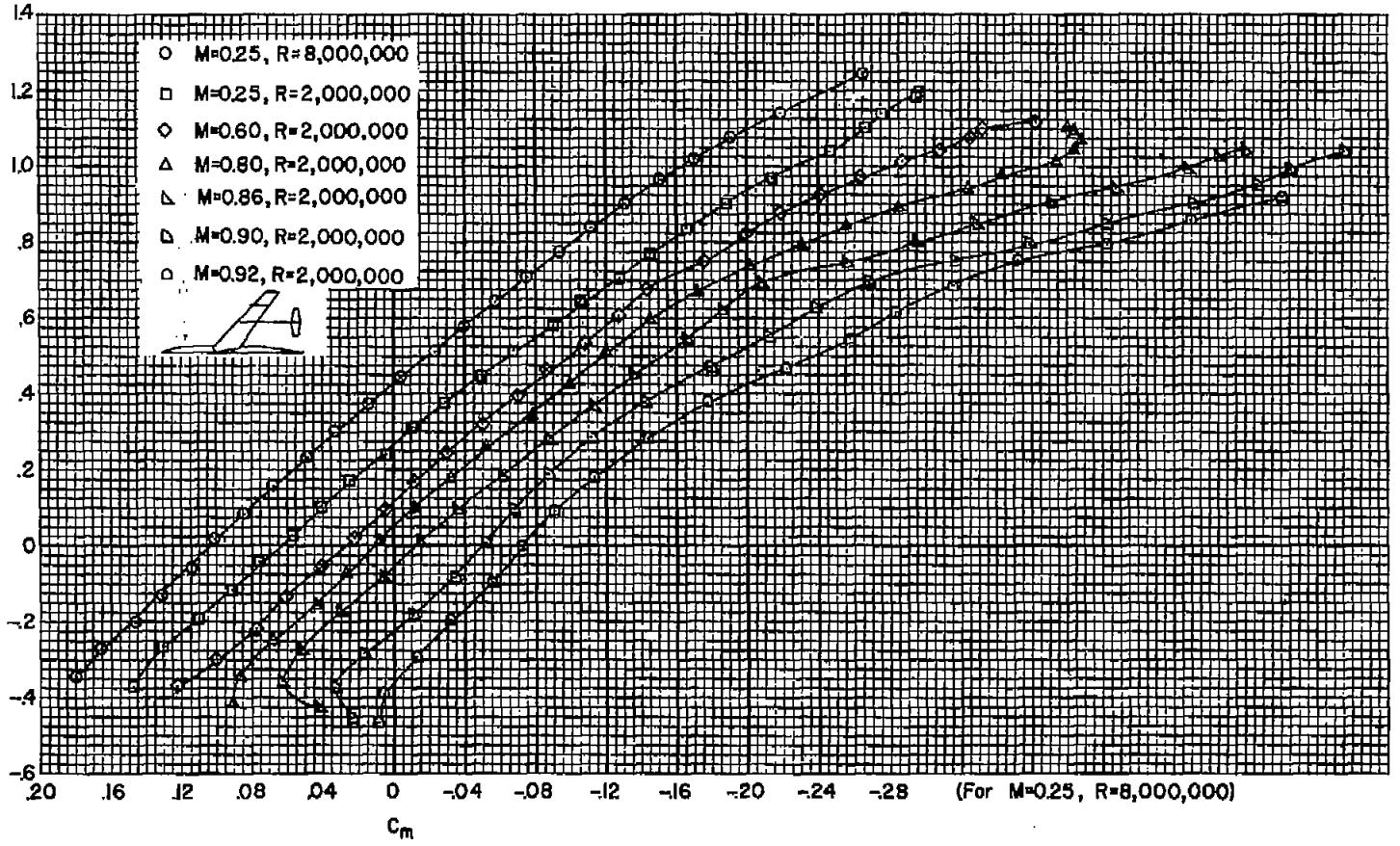

(c) C_L vs. C_m

Figure 14.- Concluded.

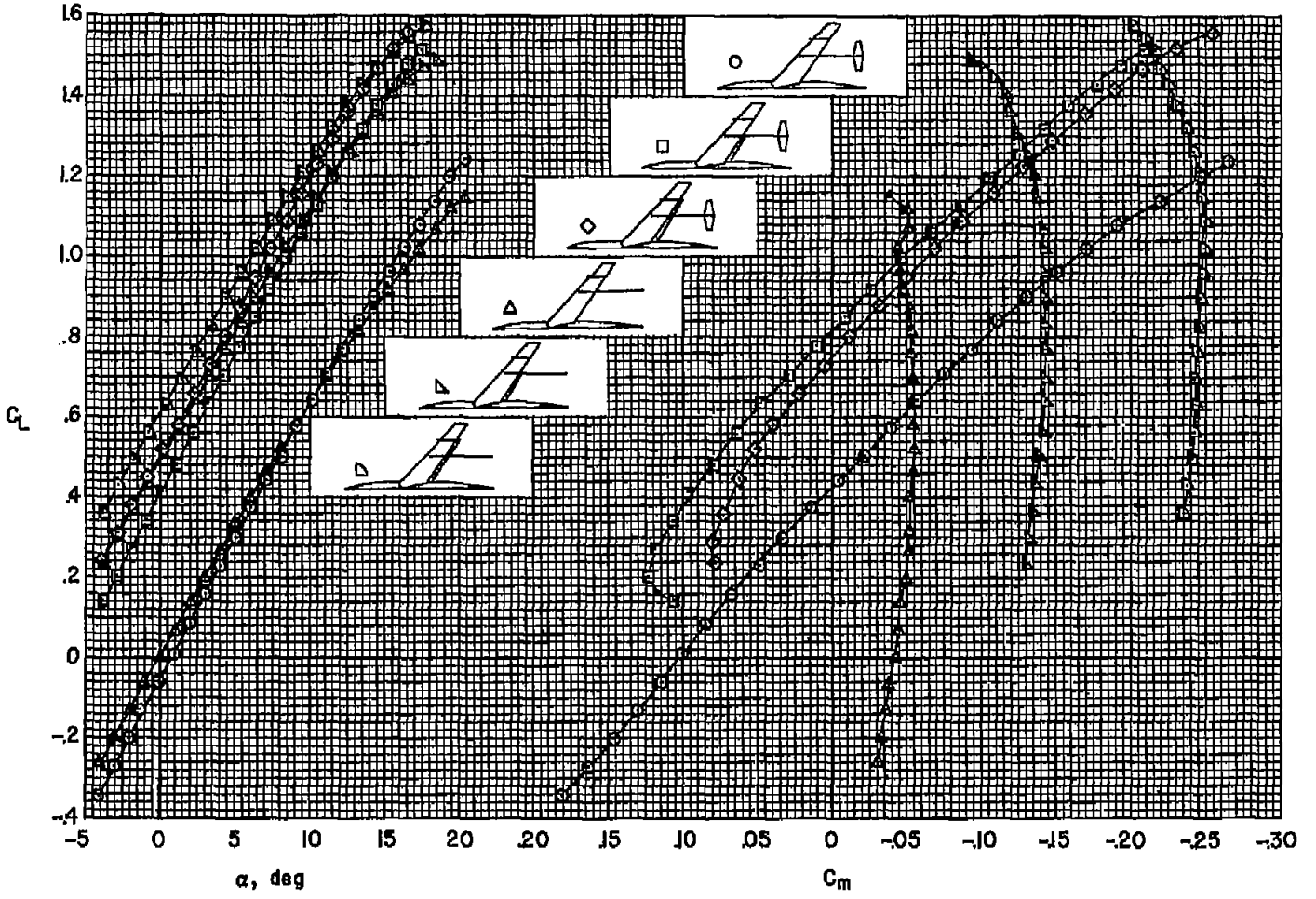

Figure 15.- The effects of flaps on the lift and pitching-moment characteristics of the model with and without the large outboard horizontal tail in low position at 0.5 b/2; M = 0.25, R = 8,000,000, $i_t = -6^\circ$.

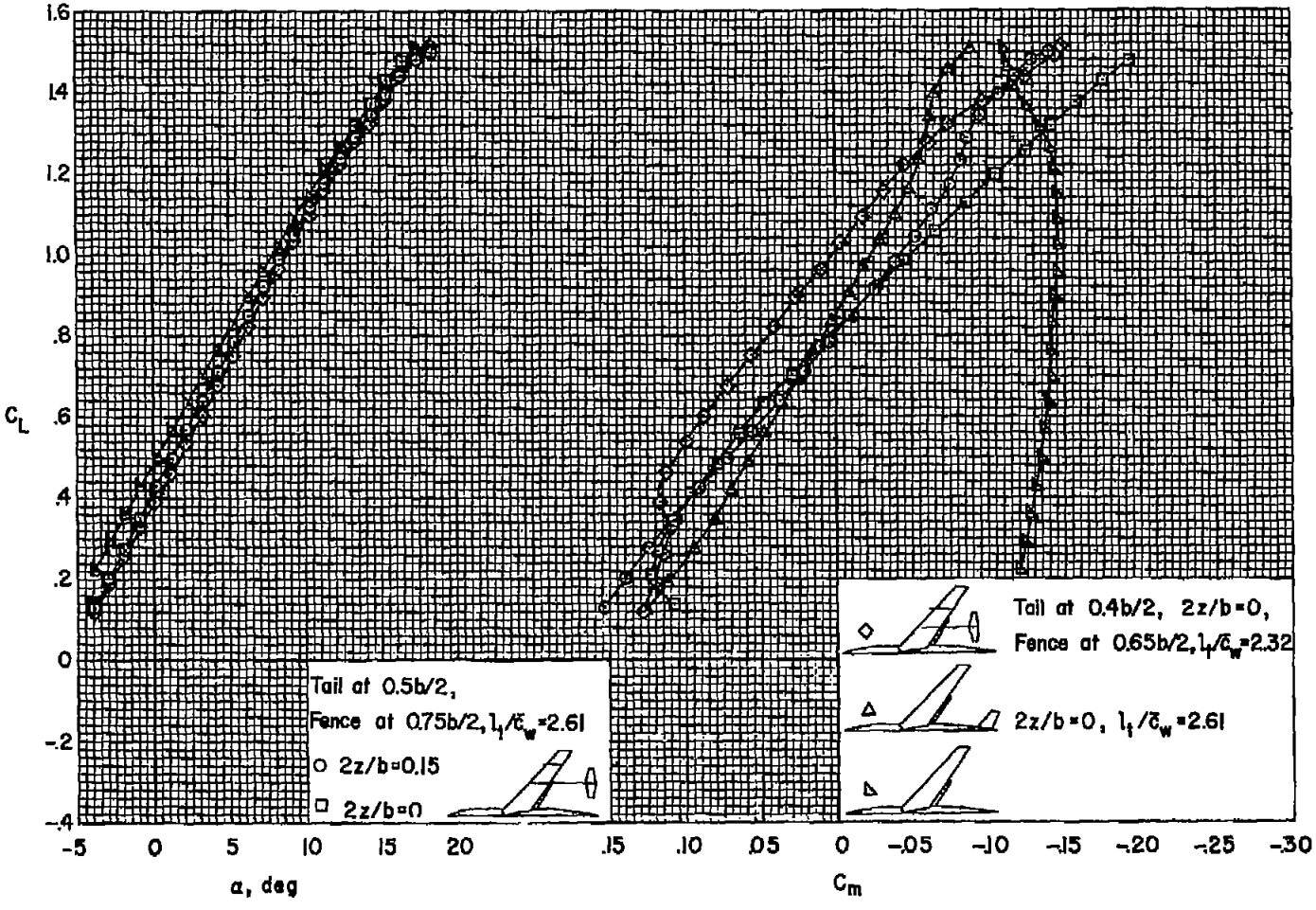

Figure 16.- The effects of tail position on the lift and pitching-moment characteristics of the model with flaps deflected; M = 0.25, R = 8,000,000, i_t = -6°.

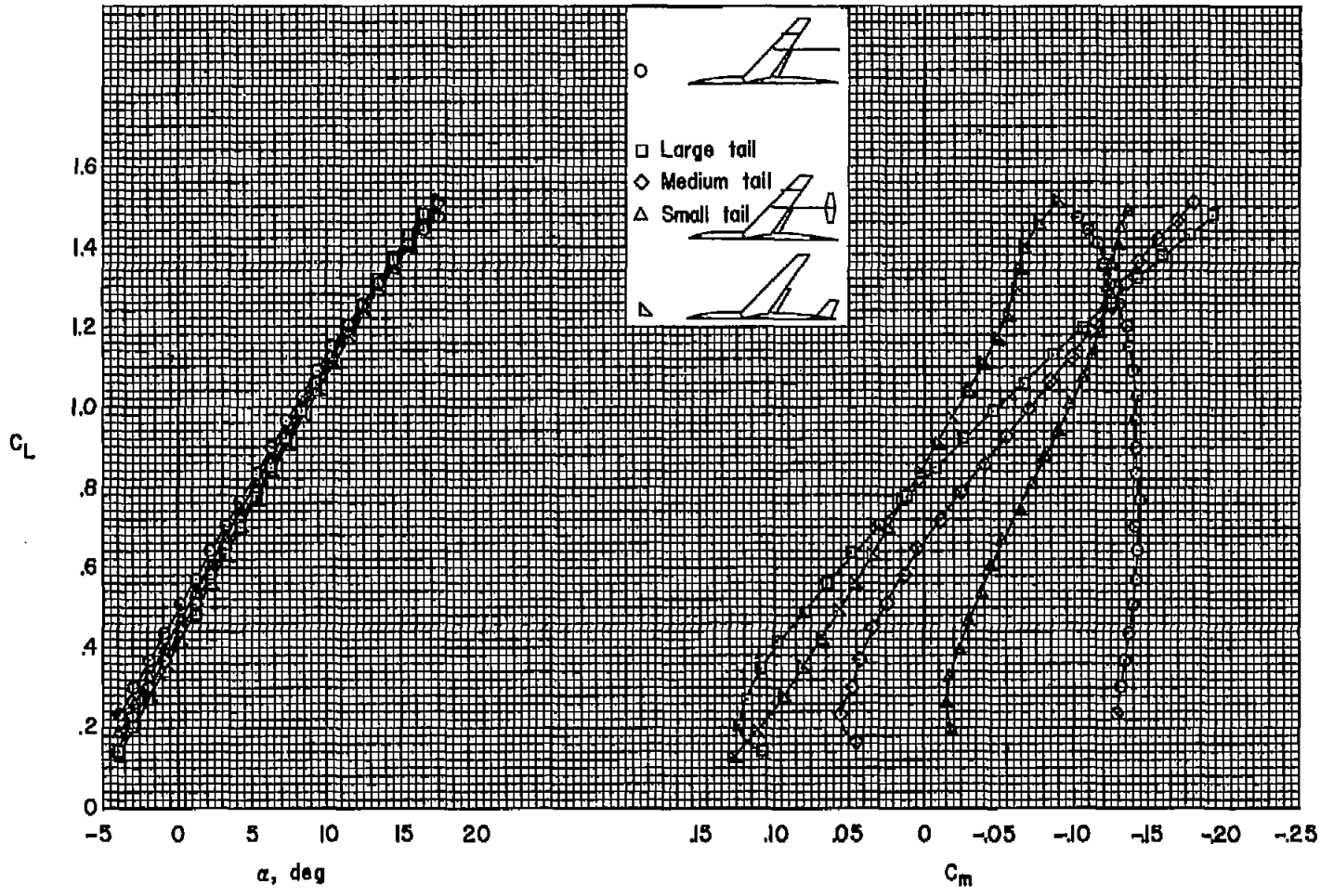

Figure 17.- The effects of tail size on the lift and pitching-moment characteristics of the model with flaps deflected; tails in low position at 0.5 b/2; $i_t = -6^\circ$, M = 0.25, R = 8,000,000.

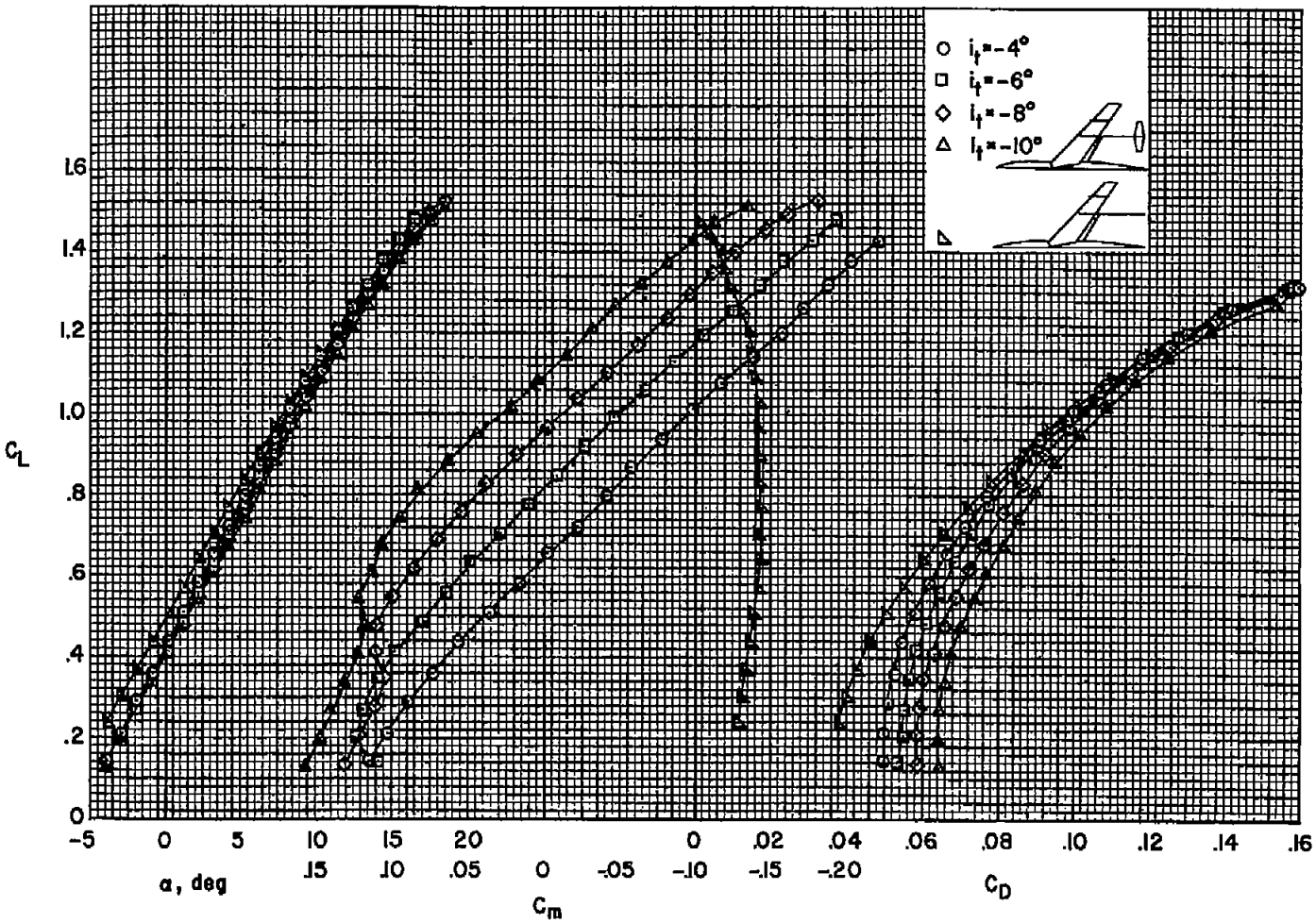

Figure 18.- The longitudinal characteristics of the model with large outboard tail at several incidences; tail in low position at 0.5 b/2; flaps deflected; M = 0.25, R = 8,000,000.

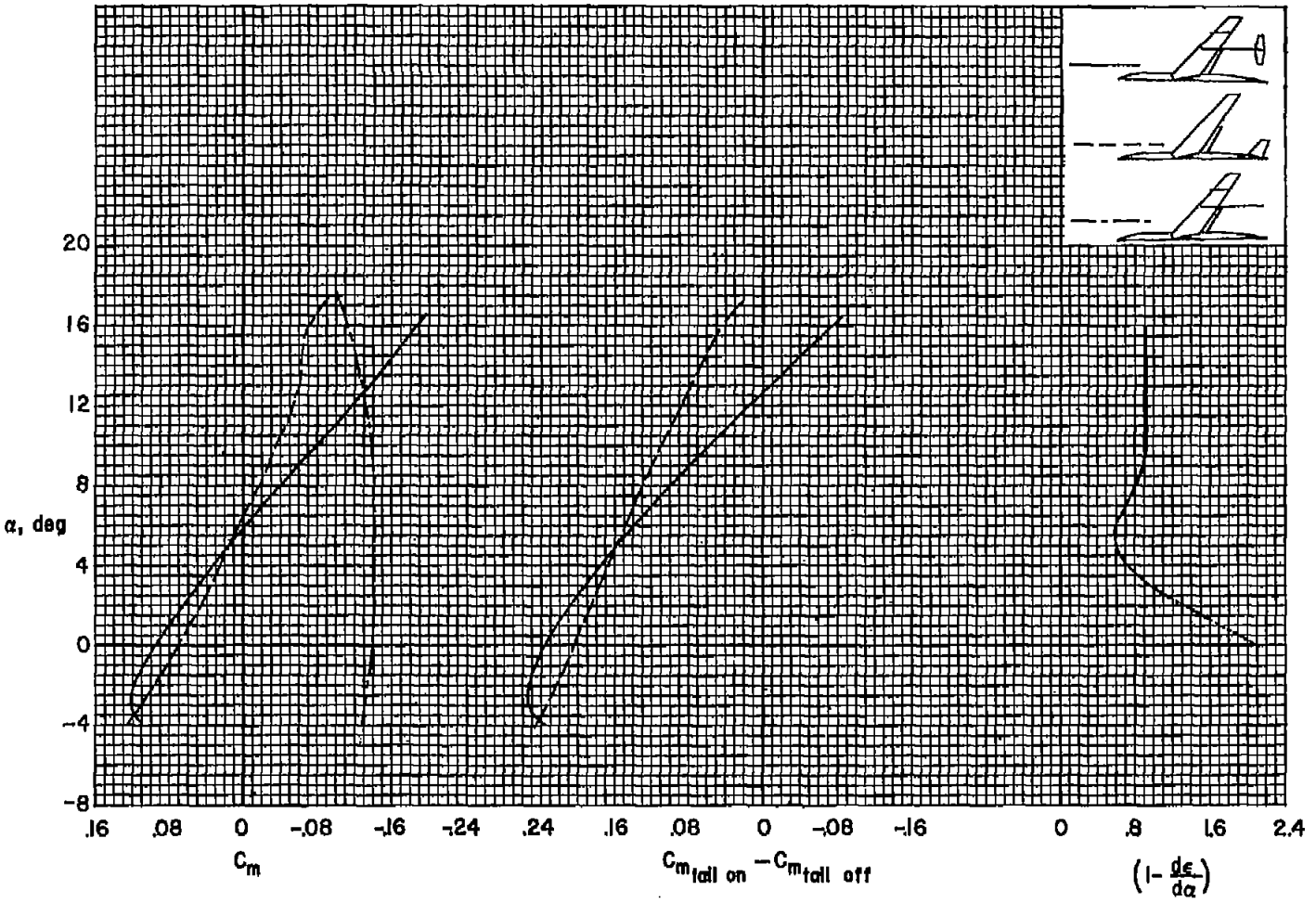

Figure 19.- The variations with angle of attack of total pitching-moment coefficient, pitching-moment coefficient due to horizontal tail, and downwash parameter for the model with a large outboard tail in low position at 0.5 b/2 and with a conventional sweptback tail; flaps deflected; M = 0.25, R = 8,000,000, $i_t = -6^\circ$.